Working Paper Series

Hervé Le Bihan, Danilo Leiva-Leon,
Matías Pacce

Underlying inflation and asymmetric risks

Abstract

We propose a new measure of underlying inflation that informs, in real time, about asymmetric risks on the outlook of inflationary pressures. The asymmetries are generated through nonlinearities induced by economic activity. The new indicator is based on a multivariate regime-switching framework jointly estimated on disaggregated sub-components of the euro area HICP and has several additional advantages. First, it is able to swiftly infer abrupt changes in underlying inflation. Second, it helps to timely track turning points in underlying inflation. Third, the proposed indicator also has a satisfactory performance with respect to various criteria relevant for inflation monitoring.

Non-technical summary

Underlying inflation –even absent a single definition agreed upon by all analysts –can be broadly defined as the persistent component in inflation. Measures of underlying inflation represent an important piece of information for the conduct of monetary policy. Central banks, such as the ECB or the Federal Reserve, typically rely on a variety of indicators of underlying inflation to make a robust assessment of inflationary pressures. Underlying inflation is for instance a key input to calibrate ECB policy tightening faced with the ongoing persistent inflationary episode (see Lagarde, 2023, Lane, 2023, Villeroy de Galhau, 2023).

Underlying inflation indicators are typically constructed either based on the exclusion of certain volatile items from the consumption basket, or based on econometric models that estimate the persistent component of inflation dynamics. Exclusion-based measures do not account for the contemporaneous contribution that volatile items -such as energy or food- may have on underlying inflation. Model-based measures tend to rely on the assumption that underlying inflation can only exhibit smooth changes over time, commonly modelled as a random walk. These characteristics can be challenged in some contexts like the current one, where the abrupt surge in energy prices has rapidly spilled over other items in the consumption basket. Against this background, this paper proposes a new measure of underlying inflation for the euro area that considers all the items of the HICP (Harmonized Index of Consumer Prices) and promptly responds to abrupt changes in inflationary pressures. The proposed measure, that is built upon a nonlinear econometric framework, is based on estimating a regime-switching model at the sectoral level, relying on special aggregates sub-indices of inflation over the sample 1999:1 to 2023:3. The resulting indicator is labeled ICARIS (Indicator of Core by Aggregating Regimes of Inflation Sub-components). We view our indicator as a relevant addition to the existing set of indicators of underlying inflation.

Our measure is able to provide not only assessments on the level of underlying inflation, but also a robust characterization of the entire distribution of this latent variable. This distribution contains valuable information that can be used for both (i) anticipating turning points in inflation and (ii) measuring asymmetric risks associated with upcoming inflationary pressures. These two features result from the assumption of state-dependence in price dynamics, where real activity informs about the transitions between regimes of inflation. Although, our framework could be easily extended for the inclusion of additional factors that might also inform on inflation risks.

In addition, we document that our measure displays a good performance when used in a real-time context and is also competitive in the forecasting arena when compared with existing underlying inflation measures. We illustrate how the indicator and associated statistics allow to timely track regime changes in underlying inflation, including during the recent inflationary episode.

1 Introduction

Underlying inflation indicators are widely used by central banks, in particular the European Central Bank (ECB) and the US Federal Reserve (Fed), in their monitoring of inflation developments and in their communication (see e.g. Ehrmann, Ferrucci, Lenza, and O'Brien, 2018 or, in the context of the recent ECB strategy review, ECB, 2021). For instance, the ECB forward guidance for interest rates between July 2021 and the eventual lift-off in July 2022, had relied, inter alia, on the observed developments of underlying inflation as a condition for lift-off (see Lane, 2021). Underlying inflation is also a key input to calibrate ECB policy tightening faced with the ongoing persistent inflationary episode (see Lagarde, 2023, Lane, 2023, Villeroy de Galhau, 2023). Underlying or "core" inflation –even absent a single definition agreed upon by all analysts –can be broadly defined as the persistent component in inflation.[1] One attractive feature of a core inflation measure, for communication purposes, is to capture in a single and replicable number the current trend in inflation, without resorting to an explicit forecast exercise. Underlying inflation is essentially an empirical concept –albeit some relations to structural macroeconomic models can be traced out– and, typically, a number of alternative indicators of underlying inflation are simultaneously used in a given institution.

Model-based indicators of underlying inflation have been typically built upon the assumption of linearity in the dynamics of prices – although there are several works that emphasize the importance of accounting for state-dependence when modelling inflation (e.g. Ascari and Haber (2022), Cavallo, Lippi, and Miyahara (2023), Klenow and Kryvtsov (2008) and Eichenbaum, Jaimovich, and Rebelo (2011)). In addition, the recent abrupt surge in energy prices and raw material prices, and the subsequent rapid pass-trough to other items in the consumption basket, challenges the assumption that underlying inflation can only exhibit smooth changes over time, that are commonly characterized by a random walk.

This paper develops an empirical model of euro area inflation, resulting in a new indicator of underlying inflation. This indicator, labeled ICARIS (Indicator of Core by Aggregating Regimes of Inflation Sub-components), is based on estimating a regime-switching model at the sectoral level, relying on special aggregates sub-indices of inflation. The indicator draws on information from all components of Consumer Price Index (CPI).[2] The approach is flexible enough to produce a level of trend inflation that can vary on a large grid of values, and to capture transitions from low to high underlying inflation regimes that can be either smooth or abrupt. These features are particularly relevant in views of the shocks to inflation during the last decade in advanced economies, and in particular to capture the possible changes in regimes following the post-covid 19 crisis, and the consequences of the invasion of

---

[1] In this paper, we use indifferently the terms underlying inflation and core inflation. We view core inflation and underlying inflation as embodying the same concept, but acknowledge that a common practice is to use "core inflation" to refer to the specific measure excluding food and energy.

[2] We here use the Harmonized Indices of Consumer Prices (HICP), published by EUROSTAT, the common measure used across countries for CPI in the euro area.

Ukraine by Russia. A main feature –that is induced by the parametric and non linear structure– of our indicator is that it also allows for a characterization of risks: at a given point in time, the outlook for inflation is predicted to be either upward or downward skewed.

Our paper is related to a large literature on core inflation –and trend inflation– indicators where three broad approaches can be distinguished. First, exclusion-based and reweighting-based measures. This type of approach has been used since the 1970s and its main idea is, based on the distribution of the different sectoral inflation rates, or COICOP subclasses, to exclude some of them from the inflation measure.[3] The most traditional exclusion-base indicator is the "inflation excluding food and energy" which permanently assigns a zero weight to both food and energy items. Alternatively, it is possible to remove at each date the items for which the inflation rate of the different classes (or sub-classes) lie in the tails of the cross classes (or sub-classes) distribution. An early reference for this kind of approach is the well known "trimmed mean" indicator of Bryan and Cecchetti (1994). Also, Lalliard and Robert (2022) propose the "fine core" that is based on trimming individual items exhibiting the largest historical volatility. Some alternative, reweighting-based measures, replace CPI weights by weights based on persistence, or by the degree of price stickiness from the micro data.

Second, trend-cycle decomposition (i.e. time series smoothing methods). Examples include the exponential smoothing approach put forward by Cogley (2002), or the unobserved component (UC) model by Stock and Watson (2007). Also, Chan, Koop, and Potter (2016) propose tailored UC models to produce bounded measures of trend inflation. In the same vein, Chan, Clark, and Koop (2018) complement UC models with exogenous information from survey expectations.[4] Also, Mertens (2016) allows the inclusion of the term structure of interest rates in a model to estimate trend inflation for the US economy.

A third set of approaches is based on models that combine time-series and the cross-section distribution of price changes, most often using factor models. A subset of this literature restricts the input variables to the different classes (or sub-classes) of inflation indices, as in Stock and Watson (2016) –a prominent recent reference which also includes an overview of the literature–. A recent indicator in this vein, for the US economy, is the Multivariate Core Trend by Almuzara and Sbordone (2022).[5] Another subset considers including other macroeconomic variables in the factor analysis (see, for instance, the euro area core inflation indicator of Cristadoro, Forni, Reichlin, and Veronese, 2005).

In the case of the euro area, on which our empirical application focuses, Ehrmann, Ferrucci, Lenza, and O'Brien (2018) summarize the underlying inflation measures typically used at the ECB, empha-

---

[3]The Classification of Individual Consumption According to Purpose (COICOP) is the international reference classification of household expenditure.

[4]A similar approach is evaluated for the case of the euro area in Bańbura, Leiva-León, and Menz (2021).

[5]Also, one prominent measure produced by the New York Fed is the Underlying Inflation Gauge (UIG) (Amstad, Potter, and Rich, 2014).

sizing two recently developed approaches. First, the so-called "super core" measure that is based on a subset of items of HICP inflation excluding energy and food that are deemed sensitive to slack. Second, the "Persistent and Common Component of Inflation" (PCCI) indicator, proposed by Bańbura and Bobeica (2020), that relies on factor models.

In relation to this large literature our approach has two main characteristics: (1) it relies on regime switches to identify periods of sustained high and low inflation, and (2) the proposed core inflation measure relies on a disaggregate, bottom-up approach. In particular, core inflation is computed by aggregating the regime-dependent persistent components over sub-indices of inflation using their corresponding weights on headline HICP.

On the methodological side, our paper is related to the literature on regime shifts as we rely on Markov-switching models. In particular, we build upon the approach of Leiva-León, Pérez-Quirós, and Rots (2020), used to analyze downside risks to the global business cycle, and propose a new decomposition of inflation into a regime-dependent persistent component and temporary fluctuations. Unlike the standard Markov-switching approach, we let each regime of inflation, either low or high, to be characterized by its unique degree of inflation strength.[6] Also, our framework allows information on real activity to inform about the transitions between regimes of high and low inflation.[7]

Our indicator comes with a number of advantages with respect to the existing measures of underlying inflation. First, the regime switching approach allows for non-linearity in inflation dynamics. To our knowledge, this is the first indicator of trend or underlying inflation built in this set-up. Incidentally, we do not assume trend inflation follows a unit root process, by contrast with an assumption often adopted in trend-cycle decompositions of inflation. Our approach is in this respect in better accordance with the non explosive inflation behavior in inflation targeting or price-stability oriented monetary jurisdictions.

Second, depending on the synchronization between the different special aggregates of inflation, the transition from (say) low underlying inflation regime to higher inflation regime could be either smooth or immediate. This is a particularly relevant feature in the current situation. In this vein, we document an asymmetric propagation pattern of euro area inflationary pressures over time. Transitions from a high- to a low-inflation regime are smooth and sequential across sub-components of HICP. Instead, transitions from low- to high-inflation regime are immediate, implying a simultaneous switch across HICP sub-components.

Third, given its nonlinear nature, our approach allows for inferences on structural breaks without the need of restricting the sample on a priori grounds, as the regimes are endogenously inferred from the data. This feature is particularly important when producing real-time inferences of underlying inflation

---

[6]Recently, Lopez-Salido and Loria (2020) have used a (standard) Markov-switching approach to analyze headline inflation regimes for the US. Although, the focus of their analysis primarily relies on quantile regressions.

[7]In doing so, we let the transition probabilities to exhibit time-variation, introduced by Filardo (1998).

during unprecedented episodes, such as the abnormally high euro area inflation rates observed since late 2021.

Most importantly, our framework can be also used to measure asymmetric tails risks associated with future underlying inflation. Such asymmetry results from the induced non-linearity in our model. This is a feature that could be of high relevance for policy in projection exercises carried out, or from the point of view of a "risk management" perspective, particularly, during periods of high uncertainty.

In addition to the above distinctive features of ICARIS, our measure is also comparable in terms of properties associated with existing euro area underlying inflation indicators. For example, it contains information from all the different components of inflation indices at any given date. Also, it has a competitive performance when used to forecast HICP inflation.[8]

While we emphasize that our model, and the associated underlying inflation measure is a reduced-form and essentially an empirical device, a brief discussion of relation with more structural macroeconomic framework or models is warranted.[9] Our approach is well suited to accommodate changes in inflation target; to acknowledging there are persistent trends in relative prices, and that the inflation dynamics is well captured by a succession of "regimes"(such as the low inflation regime in the euro area in the 2014-2020 period) without a full synchronization across sectors. We also have to acknowledge some theoretical limitations: the links between cross-inflation special aggregates indices are only captured in a simplified manner, and we do not implement the restriction that in the (very) long run, relative prices are expected to reach a steady state.

The paper is structured as follows. Section 2 introduces our model and outlines the estimation method. Section 3 presents the results obtained applying our approach to disaggregated euro area inflation. Section 4 presents our indicator of underlying inflation and investigate its properties when used in a real-time context and for risk assessment. Section 5 compares our indicator with existing indicators. Section 6 concludes.

2 A Regime-based Persistence-Noise Decomposition

A widely used approach to decompose inflation into transitory and permanent fluctuations is the unobserved component (UC) model, where the permanent component is assumed to follow a random walk and the transitory component typically behaves according to autoregressive processes.[10] Despite the usefulness of this type of decomposition, it has an important shortcoming. The persistent component

---

[8]To evaluate core inflation indicators, we rely on forecast performance, following inter alia Crone, Khettry, Mester, and Novak (2013) and Clark (2001).

[9]From a theoretical standpoint, menu cost models predict that inflation will behave non linearly, depending on the size of marginal cost shocks, see e.g. Alvarez, Lippi, and Passadore (2016).

[10]For variants of this kind of model see for example, Stock and Watson (2007) or Chan, Koop, and Potter (2013).

relies on a slow-moving process that is not able to swiftly adapt to abrupt changes in underlying inflation pressures, and precludes providing timely assessments for policy makers when needed the most. Also, inferences obtained by means of UC models are typically subject to a large amount of revisions when used in a real-time context. This section introduces a new framework to model inflation referred to as *Persistence-Noise* decomposition. The proposed modelling approach (i) takes into account the inherent nonlinear nature of the inflationary process, (ii) provides a robust estimation of inflation persistence, (iii) produces inferences of turning points in inflation, (iv) helps to quantify asymmetric risks associated with future developments of inflation, and (v) accounts for the role that covariates such a current and lagged real activity have in determining inflation dynamics.

2.1 The Model

Our empirical framework consists of decomposing the annual rate of inflation associated with each sub-aggregate of the HICP into two components.[11] The first component is designed to measure the persistence inherent in inflation dynamics. Instead, the second component refers to the temporal deviations of the observed special aggregate inflation rate from its persistent component, we refer to these deviations as noise. We assume that inflation transitions over two states of nature, defined as "low" and "high" inflation regimes. Also, we assume that the strength (weakness) of a high (low) inflation regime might change over time, implying that each regime is uniquely characterized. Accordingly, the annual inflation rate of the *i*-th special aggregate of the HICP can be expressed as follows,

$$\pi_{i,t} = \mu_{i,t} + v_{i,t}, \tag{1}$$

where $\mu_{i,t}$ denotes the persistent component and $v_{i,t}$ denotes the noisy deviations of inflation.

Estimates will be carried out at the monthly frequency. We choose to model on year-on-year inflation (the inflation measure typically of interest to policy makers) rather than monthly rates of change since seasonal patterns render the monthly inflation rate extremely noisy, and would blur identification of regimes.[12] Resulting serial correlation is accommodated through allowing for autocorrelation in the shock process $v_{i,t}$.

The persistent component of inflation is intended to shed light on two questions that apply to each special aggregate: (i) is inflation experiencing a high- or a low-inflation regime? and (ii) how strong or weak is being such a high- or a low- inflation regime? Therefore, we assume that $\mu_{i,t}$ evolves according

---

[11]We will refer hereafter to the sub-aggregates we consider as "special aggregates" as we design a specific partition of the HICP relevant for our purpose as detailed in Section 3.

[12]Official seasonally adjusted data are not available at all dis-aggregate levels of the HICP.

to the following nonlinear process:

$$\mu_{i,t} = \mu_{i0,\tau_{i0}}(1 - s_{i,t}) + \mu_{i1,\tau_{i1}} s_{i,t}, \qquad (2)$$

where $s_{i,t}$ is a discrete latent variable that dictates the state of nature of the inflation rate of the i-th special aggregate, that is, low-inflation regime, when $s_{i,t} = 0$, and high-inflation regime, when $s_{i,t} = 1$. The terms $\mu_{i0,\tau_{i0}}$ and $\mu_{i1,\tau_{i1}}$ denote the expected inflation rate during the τ_{i0}-th low-inflation regime and the τ_{i1}-th high-inflation regime, respectively, associated with the i-th special aggregate. These parameters inform about the degree of strength of inflationary pressures at a given regime. Each regime-dependent mean is treated as a random variable that is assumed to be normally distributed,

$$\mu_{i0,\tau_{i0}} \sim i.i.d. \mathcal{N}(\delta_{i0,\tau_{i0}}, \sigma^2_{i0,\tau_{i0}}), \qquad (3)$$

$$\mu_{i1,\tau_{i1}} \sim i.i.d. \mathcal{N}(\delta_{i1,\tau_{i1}}, \sigma^2_{i1,\tau_{i1}}), \qquad (4)$$

where $\delta_{i\kappa,\tau_{i\kappa}}$ and $\sigma^2_{i\kappa,\tau_{i\kappa}}$ denote the first and second moments that characterize their distribution, for $\kappa = \{0,1\}$. That is, for the i-th special aggregate, each low-inflation and high-inflation regime has its own unique mean, which is independent from the ones associated with other episodes. This is a key feature of our framework since it allows to fit regime-switching models to highly heterogeneous inflation dynamics without the need of assuming more than two regimes, which would complicate both the estimation of the model and the interpretation of the multiple inferred regimes.

For example, suppose that period t corresponds to a τ_0-th low-inflation regime, so that $s_{i,t} = 0$. In this case, the inflation rate of the i-th special component is expected to equal the low-inflation regime mean μ_{i0,τ_0}. The high-inflation regime mean μ_{i1,τ_1} has no effect: we assume that it remains the same as during the τ_1-th high-inflation regime that was right before the τ_0-th low-inflation regime, and refer to it as a "counterfactual" high-inflation mean for the corresponding period. When the τ_0-th low-inflation regime ends, its corresponding mean μ_{i0,τ_0} becomes ineffective and a new high-inflation regime mean μ_{i1,τ_1+1} determines the expected value of the inflation rate $\pi_{i,t}$.[13] To give an illustrative example, suppose that the economy begins in a high-inflation regime. Then, for $t = 1, ..., T$, the values of μ_{i1,τ_1} and μ_{i0,τ_0} described in Figure 1 would be applicable.[14]

Inferences on the value of $s_{i,t}$ provide assessment on the type of inflationary regime that the i-th special aggregate exhibits at time t. Following Filardo (1998), the latent state $s_{i,t}$ is assumed to follow a

---

[13]The notion of the "counterfactual" time-varying regime-dependent means was introduced in Eo and Kim (2016) within the context of slow moving means modelled as random walks.

[14]Given that the first episode in the illustration with simulated data corresponds to a high-inflation regime, the initial value of the "counterfactual" low-inflation regime mean μ_{0,τ_0}, prior to the beginning of the sample, can be treated as an additional parameter and estimated within the proposed algorithm.

Figure 1: Illustration of Regime Changes with Heterogeneous Means
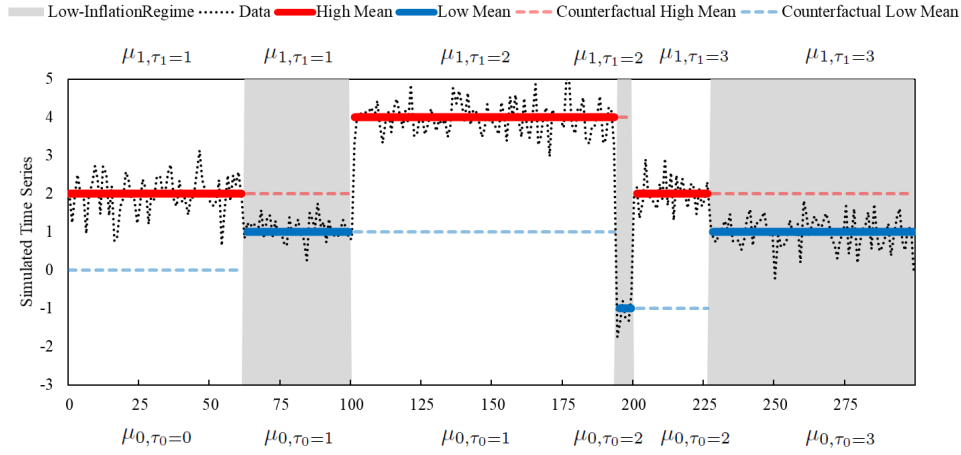
Note. The figure plots a simulated time series that exhibits regime changes with heterogeneous regime-dependent means.

first order Markov chain with a time-varying transition probability matrix given by

$$P(s_{i,t} = k | s_{i,t-1} = j, \mathbf{z}_t) = \begin{bmatrix} q_i(\mathbf{z}_t) & 1 - p_i(\mathbf{z}_t) \\ 1 - q_i(\mathbf{z}_t) & p_i(\mathbf{z}_t) \end{bmatrix}, \tag{5}$$

where $p_i(\mathbf{z}_t) = P(s_{i,t} = 1 | s_{i,t-1} = 1, \mathbf{z}_t)$ and $q_i(\mathbf{z}_t) = P(s_{i,t} = 0 | s_{i,t-1} = 0, \mathbf{z}_t)$ are the probabilities of staying in high-inflation and low-inflation regimes, respectively. The vector $\mathbf{z}_t$ represents a set of exogenous information that influences the regime transitions of inflation. Consequently, the information contained in $\mathbf{z}_t$ can be used to provide timely inference about changes in the momentum of inflation. Based on the notion of the Phillips curve, we let $\mathbf{z}_t$ contain information on contemporaneous and lagged real economic activity. We view this set-up as a parsimonious way to incorporate a common dynamics to sub-components of the HICP.

The transition probabilities are assumed to follow a latent variable version of a Probit specification, that is,

$$P(s_{i,t} = 1) = P(s_{i,t}^* \geq 0). \tag{6}$$

The latent variables $s_{i,t}^*$, for $i = 1, ..., n$, are assumed to depend on common and idiosyncratic components through the following factor structure,

$$s_{1,t}^* = \boldsymbol{\lambda}_{1,z}' \mathbf{z}_t + \lambda_{1,0} + \lambda_{1,s} s_{1,t-1} + u_{1,t}, \tag{7}$$

$$\vdots$$

$$s_{n,t}^* = \underbrace{\boldsymbol{\lambda}_{n,z}' \mathbf{z}_t}_{common} + \underbrace{\lambda_{n,0} + \lambda_{n,s} s_{n,t-1} + u_{n,t}}_{idiosyncratic},$$

with $u_{i,t} \sim i.i.d.\mathcal{N}(0,1)$ and $Cov(u_{i,t}, u_{-i,t}) = 0, \forall i$. Accordingly, the time-varying transition probabilities can be expressed as,

$$p_{i,t} = 1 - \Phi(\lambda_{i,0} - \boldsymbol{\lambda}'_{i,z}\mathbf{z}_t - \lambda_{i,s}), \tag{8}$$

$$q_{i,t} = \Phi(\lambda_{i,0} - \boldsymbol{\lambda}'_{i,z}\mathbf{z}_t), \tag{9}$$

where $\Phi(\bullet)$ makes reference to the CDF of a Normal distribution.[15]

The noise component accounts for the accumulation of disturbances induced by the computation of the year-on-year growth rate of the corresponding price sub-index. Hence, to account for this type of dynamics, we assume that $v_{i,t}$ follows an invertible moving average (MA) process,

$$v_{i,t} = \varepsilon_{i,t} + \sum_{q=1}^{Q} \theta_{i,q}\varepsilon_{i,t-q}, \quad \varepsilon_{i,t} \sim i.i.d.\mathcal{N}(0, \sigma_i^2). \tag{10}$$

Given that this decomposition is jointly applied to the different special aggregates of HICP, exhibiting substantially heterogeneous dynamics, we keep a parsimonious specification in our empirical application and set the same number of lags for all the cases, $Q = 1$.[16] This feature along with the invertibility condition, $|\theta_i| < 1, \forall i$, allows the annual inflation rate to have an alternative infinite-order autoregressive process representation, AR(∞), with time-varying mean,

$$(1 - \theta_i L + \theta_i^2 L - \theta_i^3 L + ...)(\pi_{i,t} - \mu_{i,t}) = \varepsilon_{i,t}, \tag{11}$$

where $\mu_{i,t}$ evolves according to Equation (2). Consequently, $\pi_{i,t}$ remains a non-stationary process due to the regime changes in its mean. This feature is particularly attributed to the uniqueness of $\mu_{i0,\tau_{i0}}$ and $\mu_{i1,\tau_{i1}}$, as they are locally inferred. Next, we show in detail how the regime-dependent means are estimated along with the rest of elements involved in the model.

The non-stationary nature of $\pi_{i,t}$ provides flexibility when modelling abrupt changes and unprecedented dynamics of inflation, especially, in a real-time context. Yet, its underlying persistent component, $\mu_{i,t}$, represents a purged signal that informs about the "average", or trend, inflation within a given regime, that is dictated by latent variable $s_{i,t}$.

---

[15]Previous works, such as Stock and Watson (2016), have relied on estimating the trend component of inflation in a multivariate setting by relying on common factors. In that respect, our modelling approach is similar in spirit. However, instead of capturing common movements in inflation, we let the common factors represent sources of information that, according to economic theory, influence the current and future inflation dynamics.

[16]A higher order in the moving average process can be set at the cost of increasing parameter uncertainty. In addition allowing a MA(11) process to fully accommodate the year-on-year nature of the inflation rate considered would induce severe computational complications.

2.2 Bayesian Inference

The multivariate model is estimated with Bayesian methods by relying on a Metropolis-within-Gibbs sampler. In this section, we summarize the employed estimation algorithm that provides the posterior densities associated with both parameters and latent states involved in the multivariate persistence-noise decomposition model. Let $Y = \{\pi_{1,t}, ..., \pi_{n,t}\}_{t=1}^{T}$ contain all the available data; similarly, let $S = \{s_{1,t}, ..., s_{n,t}\}_{t=1}^{T}$ and $S^* = \{s_{1,t}^*, ..., s_{n,t}^*\}_{t=1}^{T}$ be the collection of the latent regimes and latent variables, respectively. Also, let $\mu = \{\mu_{1,t}, ..., \mu_{n,t}\}_{t=1}^{T}$ contain the information on the regime-dependent means associated with high- and low-inflation regimes. All the parameters that specify the model are collected in $\Theta = \left\{ \sigma_1^2, ..., \sigma_n^2, \theta_1, ..., \theta_n, \lambda_1, ..., \lambda_n \right\}$, where $\lambda_i = (\lambda_{i,0}, \lambda_{i,z}, \lambda_{i,s})$, for $i = 1, ..., n$. Given data Y and prior distributions for the parameters contained in vector Θ, we rely on the following iterative procedure to generate L draws of $\{\Theta^{(l)}, S^{(l)}, S^{*(l)}, \mu^{(l)}\}_{l=1}^{L}$.

> *Step 1:* Given Y, $S^{(l-1)}$, $S^{*(l-1)}$, and $\mu^{(l-1)}$, generate $\Theta^{(l)}$ using the Gibbs sampler with a Metropolis step.
>
> > *1.1:* Draw $\sigma_i^{2(l)}$, for $i = 1, ..., n$, by using a conjugate Inverse Gamma prior distribution.
> >
> > *1.2:* Draw $\theta_i^{(l)}$, for $i = 1, ..., n$, with a Metropolis step by using a Uniform prior distribution, following Chan (2013).
> >
> > *1.3:* Draw $\lambda_i^{(l)}$, for $i = 1, ..., n$, by using a conjugate Normal prior.
>
> *Step 2:* Given Y, $S^{(l-1)}$, $\mu^{(l-1)}$ and $\Theta^{(l)}$, generate $s_{i,t}^{*(l)}$, for $i = 1, ..., n$, by applying the approach proposed in Filardo (1998).
>
> *Step 3:* Given Y, $S^{*(l-1)}$, $\mu^{(l-1)}$ and $\Theta^{(l)}$, generate $s_{i,t}^{(l)}$, for $i = 1, ..., n$, by applying the algorithm proposed in Kim and Nelson (1999).
>
> *Step 4:* Given Y, $S^{(l)}$, $S^{*(l-1)}$, and $\Theta^{(l)}$, generate $\mu_{i,t}^{(l)}$, for $i = 1, ..., n$, by applying a modified version of the algorithm proposed in Leiva-León, Pérez-Quirós, and Rots (2020).

The algorithm proposed in Leiva-León, Pérez-Quirós, and Rots (2020) is designed for inferring business cycle phases of heterogeneous magnitude with data expressed on month-on-month growth rates. However, the employed procedure cannot be directly extrapolated to the analysis of year-on-year inflation rate dynamics. In what follows, we show in detail how to implement *Step 4* of the algorithm proposed in this paper. Details on *Step 1*, *Step 2* and *Step 3* of the algorithm along with the information on the prior distributions are presented in Appendix A.

For the i-th special aggregate of the HICP, we apply the partition of the time domain into the low-inflation regimes, $\tau_{i0} = 1, ..., N_{i0}$, and high-inflation regimes, $\tau_{i1} = 1, ..., N_{i1}$, as dictated by the current realization of the state indicator $S^{(l)}$, and treat each episode separately. Then, for each individual episode,

we sample its corresponding inflation mean by only using the information associated with such time span, defined by, $\pi_{\tau_{i0}} = \{\pi_{i,t}\}_{t \in \tau_{i0}}$ and $\pi_{\tau_{i1}} = \{\pi_{i,t}\}_{t \in \tau_{i1}}$. In doing so, we use the diffuse normal prior distribution $\mathcal{N}(a_\kappa, b_\kappa)$, which combined with the likelihood yields the posterior density $\mathcal{N}(\delta_{i\kappa,\tau_{i\kappa}}, \sigma^2_{i\kappa,\tau_{i\kappa}})$, with,

$$\sigma^2_{i\kappa,\tau_{i\kappa}} = \left(b_\kappa^{-1} + \frac{1}{\sigma_i^2} \mathbf{1}'_{\tau_{i\kappa}} (\mathbf{H}_{\tau_{i\kappa}} \mathbf{H}'_{\tau_{i\kappa}})^{-1} \mathbf{1}_{\tau_{i\kappa}} \right)^{-1}, \tag{12}$$

$$\delta_{i\kappa,\tau_{i\kappa}} = \sigma^2_{i\kappa,\tau_{i\kappa}} \left(b_\kappa^{-1} a_\kappa + \frac{1}{\sigma_i^2} \mathbf{1}'_{\tau_{i\kappa}} (\mathbf{H}_{\tau_{i\kappa}} \mathbf{H}'_{\tau_{i\kappa}})^{-1} \pi_{\tau_{i\kappa}} \right), \tag{13}$$

where $\mathbf{1}_{\tau_{i\kappa}}$ denotes a vector of ones of length equal to the number of observations in $\pi_{\tau_{i\kappa}}$, while $\mathbf{H}_{\tau_{i\kappa}}$ is a square matrix of size equal to the number of observations in $\pi_{\tau_{i\kappa}}$, and defined by

$$\mathbf{H}_{\tau_{i\kappa}} = \begin{pmatrix} 1 & 0 & 0 & \cdots & 0 \\ \theta_i & 1 & 0 & \cdots & 0 \\ 0 & \theta_i & 1 & \cdots & 0 \\ \vdots & & & \ddots & \vdots \\ 0 & 0 & \cdots & \theta_i & 1 \end{pmatrix}, \tag{14}$$

for $\kappa = \{0, 1\}$. Note that the role of the band matrix $\mathbf{H}_{\tau_{i\kappa}}$ is "whitening" the serially correlated innovations induced by the year-on-year growth rate of the price index. The posterior density is then used to generate draws of $\mu_{i0,\tau_{i0}}$ and $\mu_{i1,\tau_{i1}}$, as described in equations (3) and (4), respectively. To avoid problems of label switching, we follow Leiva-León, Pérez-Quirós, and Rots (2020) and identify regimes of high and low inflation by constraining the draws of the regime-dependent means at each iteration of the algorithm. In particular, they have to comply with the following two restrictions:

Restriction 1 : $\mu_{i1,\tau_{i1}} > \mu_{i0,\tau_{i0}}$

Restriction 2 : $\begin{cases} \mu_{i1,\tau_{i1}} > \mu_{i0,\tau_{i0}-1}; \text{ if the sample begins with a high-inflation regime} \\ \mu_{i0,\tau_{i0}} < \mu_{i1,\tau_{i1}-1}; \text{ if the sample begins with a low-inflation regime.} \end{cases}$

Restriction 1 constrains means associated with high-inflation regimes to be higher that means associated with low-inflation regimes. However, since the definition of what is "high" and "low" changes over time, we need Restriction 2 to ensure this intertemporal condition.

3 Nonlinear Persistence of Disaggregated Inflation

In this section, we apply our model to the different sub-components of HICP and document a large amount of heterogeneity in terms of inflation persistence. To estimate the regime-switching model at the

disaggregated level, we rely on HICP inflation data at monthly frequency and broken down by "type of product" into 11 specific categories, which are related to some "special aggregates" indices of inflation published by EUROSTAT. This breakdown is associated to the 4-categories typically used by the ECB for analytical purposes: "energy", "food", "Non-energy industrial goods", and "services", but goes to a further level of disaggregation. The breakdown we use has the advantage that all considered sub-components are relatively similar in terms of their HICP weights, which is an important feature for the computation of the ICARIS indicator in next section.[17] If the weight of one of the special aggregate stands out, this could make the indicator bias towards the persistent dynamics of that aggregate.

Table 1 shows the 11 specific aggregates (or sub-components) we consider, as well as theirs weights and some descriptive statistics associated with our sample period –January 1999 to March 2023. The average HICP weight over the specific sub-components is (by construction) 9.1 percent. Special aggregate "processed food, including alcohol and tobacco" is the one with the higher weight (15.5%), while "services related to communication" is the one with the lower one (2.2%). There is a high degree of heterogeneity between the different special aggregates both, regarding the mean and the standard deviation of the inflation rates. "Energy" and "Unprocessed Food" are the sub-components that have the highest average inflation rate (4.98% and 2.48%, respectively), while there is one special aggregate that exhibits negative average inflation rate, "services related to communication" (-1.82%). Regarding the volatility of the inflation rates across special aggregates, as expected, "energy" and "food" related items are the more volatile ones. For this reasons, these two items are typically removed when computing the exclusion-based measures of core inflation.

Regarding the information driving the time variation in the transition probabilities, we proxy real activity with the year on year growth rate of euro area Industrial Production Excluding Construction, x_t. In particular, we let the transition probabilities be potentially influenced by current and past real economic activity and let $\mathbf{z}_t = (x_t, x_{t-1}, ..., x_{t-p})'$, with $p = 11$.

We apply the model in equations (1)-(10) to the HICP special aggregates listed in Table 1. Figure 2 displays the persistent component of euro area inflation at the disaggregated level, pointing to a substantial amount of heterogeneity both over time and across categories. The estimates show that the proposed framework is flexible enough to adapt to the wide variety of inflationary dynamics embedded in the different types of goods and services.

Regime changes in some special aggregates, such as "Non-energy Durable Goods", are more recurrent than in others, as in "Services: Housing".[18] Also, the evolving magnitudes of the persistent compo-

---

[17]We do not consider the disaggregation by COICOP categories as at the division levels categories merge items that belong to quite different economic structures and inflation dynamics; e.g. "Transports" would include both purchases of cars and purchases of gasoline.

[18]The probabilities of low-inflation regime for each special aggregates of HICP are reported in Figure B-1. Note that it is uncommon for all the sub-components to be in the same type of inflation regime at the same time. During the last part of the sample almost all the aggregates face a high-inflation regime with a high probability. The "services related to miscellaneous"

Table 1: HICP and special aggregates: weights, mean and volatility

Aggregate	Special aggregate	Weights	Average inflation rate (%)	standard deviation
HEADLINE INFLATION	——-	100	1.98	1.67
FOOD	Processed food including alcohol and tobacco	15.48	2.46	1.95
	Unprocessed food	4.50	2.48	2.61
ENERGY	Energy	10.23	4.98	9.74
SERVICES	Related to communication	2.23	−1.82	1.92
	Related to housing	9.52	1.84	0.49
	Related miscellaneous	9.23	2.11	1.00
	Related to recreation	15.25	2.45	1.31
	Related to transport	7.31	2.45	0.49
NON-ENERGY INDUSTRIAL GOODS (NEIG)	Durables	9.49	0.26	1.29
	Non-durables	6.86	1.62	1.03
	Semi-durables	9.91	0.73	1.06

Note: The descriptive statistics are based on monthly year-on-year growth rates. The sample corresponds to 1999M1-2023M03. The weights correspond to the year 2023.

nent of some categories are more asymmetric than others. For example, "Processed food" exhibits quite different magnitudes across high-inflation regimes and similar magnitudes across low-inflation regimes, while "Services: Recreation" displays relatively similar magnitudes both across high- and low-inflation regimes, with exception of the last part of the sample.

Given the flexible nonlinearity embedded in the proposed model, the estimated persistent component of some special aggregates of HICP promptly reacts to recent unprecedented developments induced inter alia by the war in Ukraine. In particular, items "Non-energy: Durables" and "Non-energy: Nondurables" goods exhibited dynamics consistent with a structural break in early 2022.

The timeliness of the inferences on regime changes in inflation along with assessments on its associated strength might be key for policy makers. Our approach proves to be robust when employed in a real-time context. The persistent components of the special aggregates computed only with information available up to the time of estimation are reported in Figure B-3, placed in Appendix B for the sake of space. The real-time estimates show similar dynamics to the ones obtained with the full sample, this is the case for all especial aggregates and time spans.[19]

item is specific, having shown a relatively steady year-on-year inflation rates since 2008 without increasing significantly in the first half of 2022. This category includes items related to education, health, care of child and elderly people. Illustrating such heterogeneity, Figure B-2 plots the probability of low-inflation regime weighted across special aggregates.

[19]Also, the underlying probabilities of low-inflation regime for the special aggregates of HICP are plotted in Figure B-4 of the same appendix.

Figure 2: Persistent Component of HICP Special Aggregates
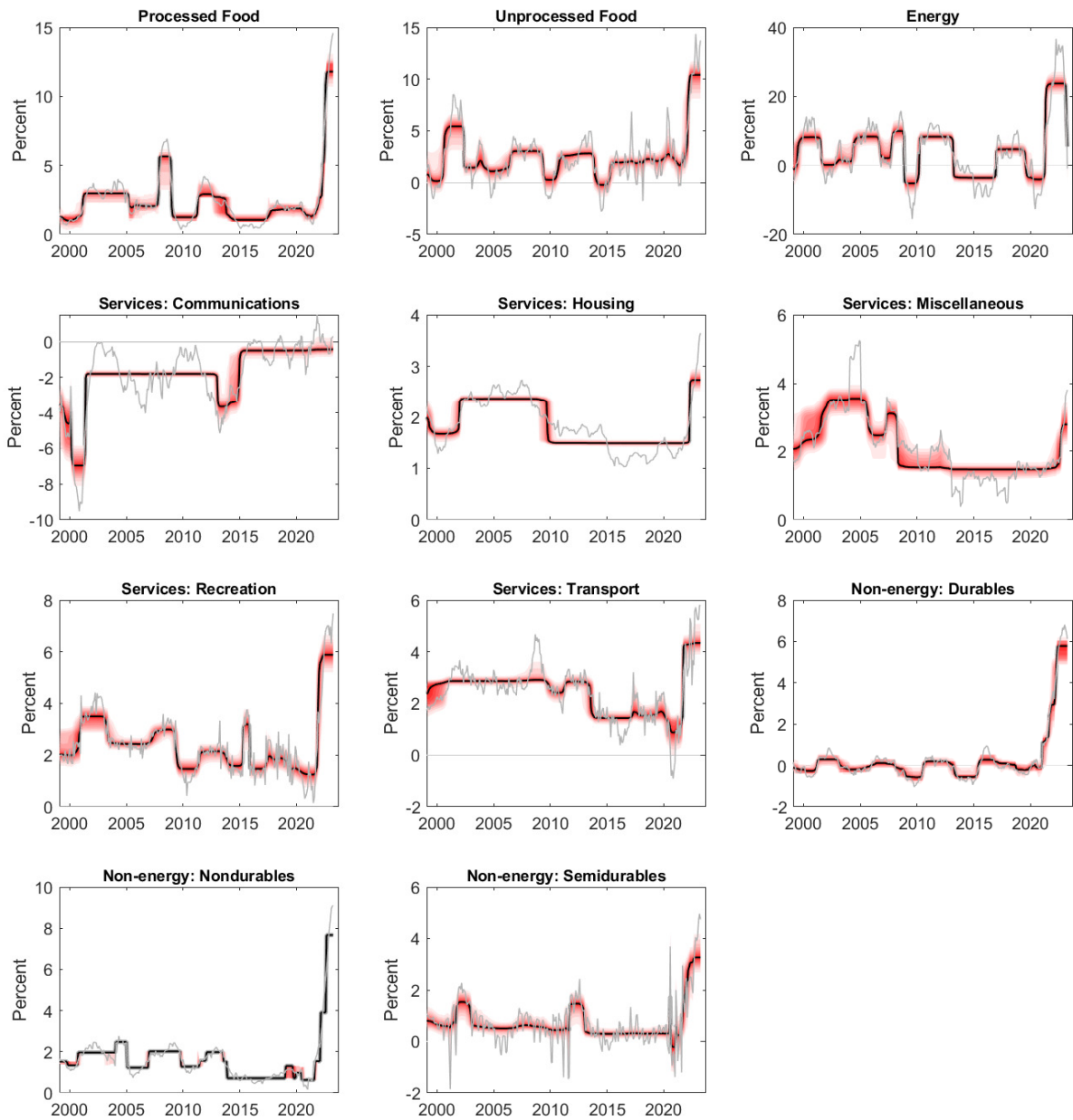
Note. The figure plots the persistent component of inflation associated with the different special aggregates of HICP. The persistent components are obtained with the proposed regime-switching model. The red area makes reference to the posterior density and the black lines its median. Each chart also plots the year-on-year growth rate of the corresponding sub-component price index for reference purposes (solid gray lines). The sample covers 1999:01-2023:03.

4 A Measure of Underlying Inflation

4.1 The ICARIS

We construct our indicator of underlying inflation averaging the persistent components associated with all the special aggregates of HICP. Hence, the ICARIS can be defined as:

$$\pi_t^{Core} = \sum_{i=1}^{N} \omega_{i,t} \mu_{i,t}, \tag{15}$$

where $\mu_{i,t}$ refers to the persistent component of the special aggregate inflation index i, as defined in Equation (2), and $\omega_{i,t}$ denotes the weight of the same special aggregate employed in the construction of the HICP. Note that the HICP weights are time varying, changing every year in January and staying constant over the year. Such an approach is in the spirit of Stock and Watson (2016), who also compute aggregate trend inflation as a weighted average of the trend inflation rates (modelled as random walks) of seventeen components of the Personal Consumption Expenditure (PCE) price index for the US.

Chart A of Figure 3 plots our measure of core inflation. The ICARIS is characterized by a strong persistence induced by the Markov chains upon which it is constructed. This is an appealing feature as this underlying inflation measure is not influenced by erratic movements often displayed in the inflation rates of special aggregates. Despite its persistence, the ICARIS is able to rapidly adjust to new inflation environments. For example, this is the case when the euro area transitioned from a sustained period of high to a sustained period of low inflation over the course of 2013. Based on these two features, our measure of underlying inflation can be also interpreted as a "locally inferred trend inflation", since it measures the average strength of inflation, but taking into account different states of nature.[20]

Chart B of Figure 3 plots the historical contribution of each HICP sub-component to the ICARIS, based on Equation (15). At every time period, the contribution of each sub-component depends on three elements: (i) the inference on its inflationary state, measured by the latent variable $s_{i,t}$, (ii) its inflationary strength, measured by the corresponding regime-dependent mean μ_i, and (iii) its importance in the consumption basket, measured by $\omega_{,it}$.[21] A key advantage of the ICARIS is that it accounts for all sub-components of HICP, unlike exclusion measures of core inflation that omit information from energy and food categories. These two sub-components typically play a relevant role in driving underlying inflationary pressures. This is particularly the case in the recent context, as the historical decomposition of the ICARIS points out.

---

[20]In principle, this indicator of underlying inflation could be affected by transitory measures such as change in the VAT rate due to the computation of the year-on-year changes in the price indices. However, this concern is alleviated in the case of the euro area, since fiscal measures such as VAT rates are not synchronized across countries. Hence, changes in VAT are not likely to induce a quantitatively sizable movement in the area wide inflation rate. Besides, note that some standard core inflation measures like inflation excluding food and energy (or even trimmed means) are themselves prone to temporary shocks following such indirect tax changes.
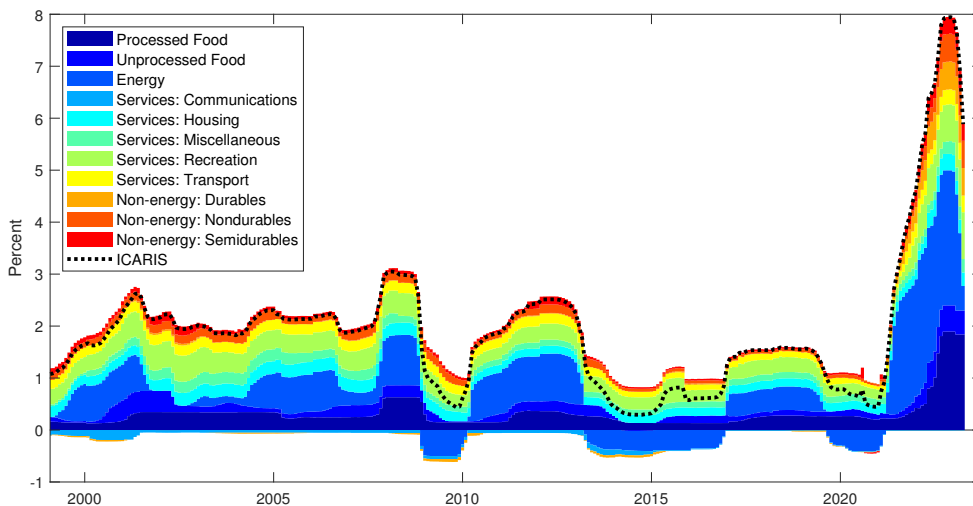
[21]For reference purposes, Figure B-5 of Appendix B reports the contribution of each special aggregate to HICP growth.

Figure 3: Indicator of Core by Aggregating Regimes of Inflation Sub-components

(a) ICARIS
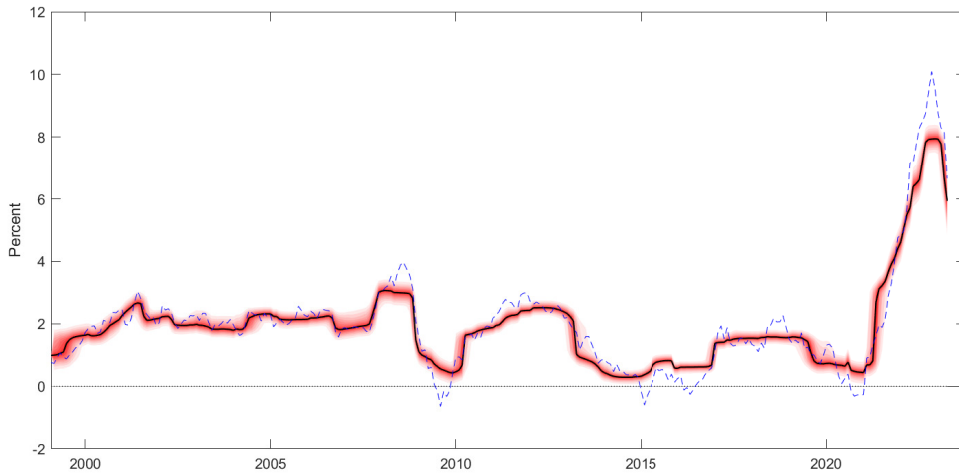
(b) Historical Decomposition

 Note. Chart (a) plots the proposed measure of core inflation. The red area makes reference to the posterior density and the black line its median. The ICARIS is obtained as a weighted average across the persistent components of inflation associated with the special aggregates of HICP. The HICP euro area inflation is also plotted with the dashed blue line, for reference purposes. Chart (b) shows the historical contribution of each special aggregate to the computation of the ICARIS. The sample covers 1999:01-2023:03.

A feature worth to be noticed is the increasing role of non-energy industrial goods (NEIG) in explaining the ICARIS during the last part of the sample. The persistent component associated with the NEIG special aggregates "Durables" and "Nondurables" have historically remained relatively stable until mid-2021, when started to register unprecedented levels (see Figure 2). This unusual behavior might be the reflection of the effect of supply bottlenecks in combination with record high energy prices. Other salient features are the stabilization of underlying inflation since the late 2022 and the abrupt decline in March 2023, induced by the fall in the persistent component of energy prices, as shown in Figure 2.

4.2 Real-timeliness

Since the probability of being in each inflation regime and the level of the permanent component in the corresponding inflation regime needs to be re-estimated each time a new observation is included for monitoring purposes, there is potential for major revisions of ICARIS. In order to study this possibility, we recursively estimate the ICARIS expanding the window by one month at a time for the last ten years of the sample under consideration. Hence, the first estimated vintage runs from January 1999 to April 2013, the second from January 1999 to May 2013 and we continue to expand the window until the entire sample, from January 1999 to March 2023, is covered. Figure B-6, placed in the Appendix B for the sake of space, plots all the estimated vintages –120 in total–. Until mid-2021, before the latest surge in inflation, ICARIS shows no major revisions, pointing to our proposed measure of underlying inflation as a robust estimate. As expected, since the second half of 2021 revisions have been more frequent. This reflects the recent acceleration of inflation, a pattern almost any model will have difficulty to predict. In this context, ICARIS has been adapting to the new information and raising the estimated permanent component accordingly.

Next, we analyze the properties of the posterior distribution of ICARIS obtained in real time and evaluate its usefulness to anticipate turning points in inflation. For reference purposes, we define regimes of high and low inflation in real time. In doing, so we apply a univariate version of our regime switching model to *aggregate* headline HICP inflation.[22] When the estimated regime probability of low inflation is higher than one half, that period is defined as a low-inflation regime. Otherwise, it is defined as a high-inflation regime.[23] Note that the employed dating of inflation regimes does not have revisions as it is computed in real time, in the spirit of the procedure followed when dating recessions by the NBER Business Cycle Dating Committee. The estimates infer two episodes of sustained low inflation in the euro area, the first one occurred between 2013 and 2017, and the second one between 2020 and 2021.

Figure 4 plots the real-time sequence of statistics of the posterior distribution of the ICARIS. Chart A plots its median that corresponds to the level of the indicator discussed above, and that we defined as the "real-time ICARIS". This is a nonlinear measure of underlying inflation computed only with the information available at the time of estimation and that has no revisions. Note that the real-time ICARIS peaked in 2023:02, signaling the beginning of a potential downward trend in underlying inflation, which might be key for policy makers to keep monitoring.

Chart B of Figure 4 plots the variance of ICARIS that displays substantial time-variation. Note the variance reflects both the "cross sector" dispersion across the persistent components in the respective

---

[22]As the estimated regimes are used only for reference purposes, we keep the univariate specification parsimonious and assume constant, instead of time-varying, transition probabilities associated with the Markovian latent variable that dictates the inflation regimes.
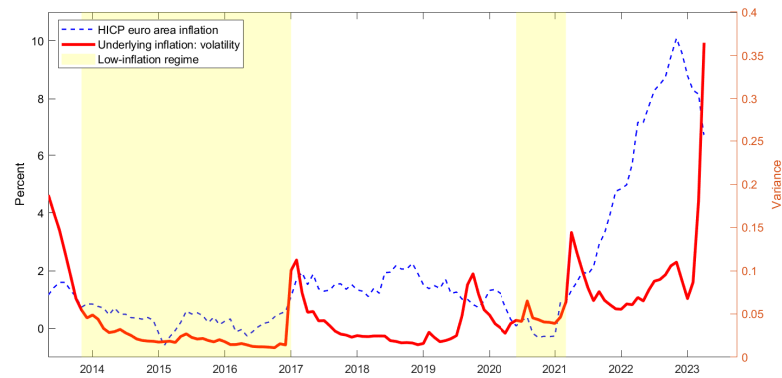
[23]The real-time probability of low-inflation regime is shown in Figure B-7 of Appendix B.
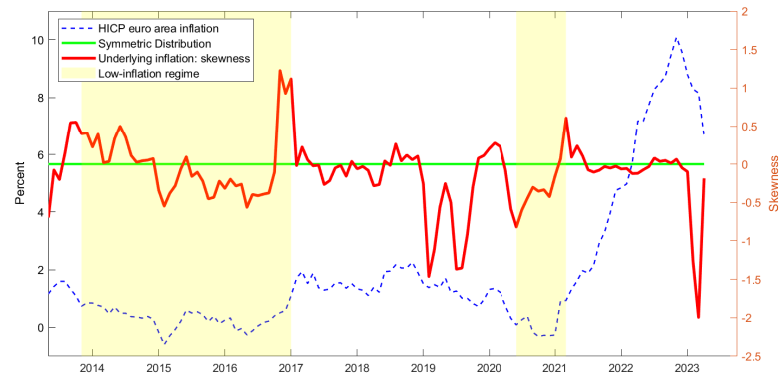
Figure 4: ICARIS in Real Time

(a) Level
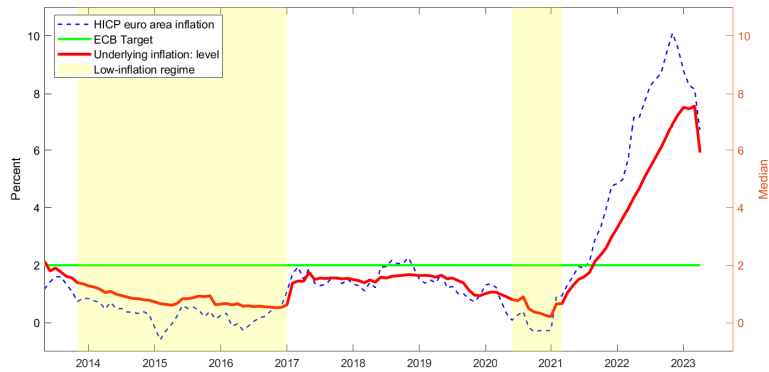
(b) Uncertainty

(c) Asymmetry

Note. Chart (a) plots the median of the posterior density of the ICARIS, estimated in a real-time fashion, that is, using only the amount of information available at the time of estimation. Chart (b) plots the variance of the posterior density of the real-time ICARIS for each point in time (right axis). Chart (c) plots the skewness of the posterior density of the real-time ICARIS for each point in time (right axis). In all charts, the HICP euro area inflation is also plotted with the dashed blue line, for reference purposes (left axis). The yellow area makes reference to low-inflation regimes, defined by a real-time probability of low inflation higher than 0.5 according to the estimates in Figure B-7. The sample covers 2013:04-2023:03.

sectors, and the "within sector" uncertainty attached to the estimation of each special aggregate persistent component. Interestingly, while this is not a property imposed by the proposed framework, transitions from one regime of inflation to another occur gradually across sub-components, that is why the variance exhibits sustained increases prior to such transitions. The evolving dispersion of the distribution of the

ICARIS can be also interpreted as the degree of internal decoupling of inflationary pressure across the items in the consumption basket. Note that upward pressures –transitions from low- to high-inflation regimes– are rapidly spread across items, while downward pressures –transitions from high- to low-inflation regime– take slightly more time to materialize. This feature is reflected in the asymmetric jumps observed in the evolving cross-sectional volatility of ICARIS in that increases take place faster that declines. Also, when comparing the spikes that the variance of the ICARIS distribution, referred to as its uncertainty, exhibits over time with the dating of headline inflation regimes, we can see a closely related pattern. Increases in the uncertainty embedded in ICARIS helps to anticipate turning points in headline inflation in real time.

On top of time-varying dispersion of the distribution of underlying inflation, ICARIS is able to produce evolving asymmetries in that distribution, which can be measured by its skewness. This is a feature that linear models are by construction not able come along with. In particular, an important aspect is that the sign of the skewness varies over time, as indicated in Chart C of Figure 4. Prior to the transition from low- to high-inflation regime of 2017, the skewness of ICARIS displayed significantly positive values, pointing to upward pressures in underlying inflation. Conversely, the ICARIS skewness exhibited mostly negative values prior to the transition from high- to low-inflation regime of 2020 signaling upcoming downward underlying inflationary pressures. In the recent observations prior to March 2023, despite the elevated level of underlying inflation, and the high background uncertainty, our indicator suggested a negative skewness of ICARIS.

To provide a more concrete illustration of the type of information contained in the evolving skewness of the ICARIS, Figure 5 plots the posterior densities at several selected dates. On the verge of the transitions to a low-headline inflation regime (as in 2019), the distribution becomes left-skewed, pointing to downside risks. Conversely, prior to the transitions to a high-headline inflation regime (as in 2016 or 2021), the distribution becomes right-skewed, consistent with upside risks. This is an indication that the ICARIS provides relevant real-time information about the risks of transitioning from one regime of headline inflation to another. The very last data point in our sample (March 2023) suggests a downward shift in underlying inflation: it was precedented in January and February by distributions of the ICARIS that were skewed to the left.

4.3 Risk Assessment

A more comprehensive approach to risk assessment relies on considering the current trend and direction of underlying inflation, as compared to the contemporaneous value of the indicator. By construction, non model-based approaches such as exclusion-based measures (e.g. the trimmed means) do not come by themselves with an indication of the current short or medium term trend. Typical trend-cycle decom-

Figure 5: Posterior Densities of ICARIS in Real Time for Selected Periods

(a) From low- to high-inflation regime in 2016

(b) From high- to low-inflation regime in 2019

(c) From low- to high-inflation regime in 2021

(d) Early 2023
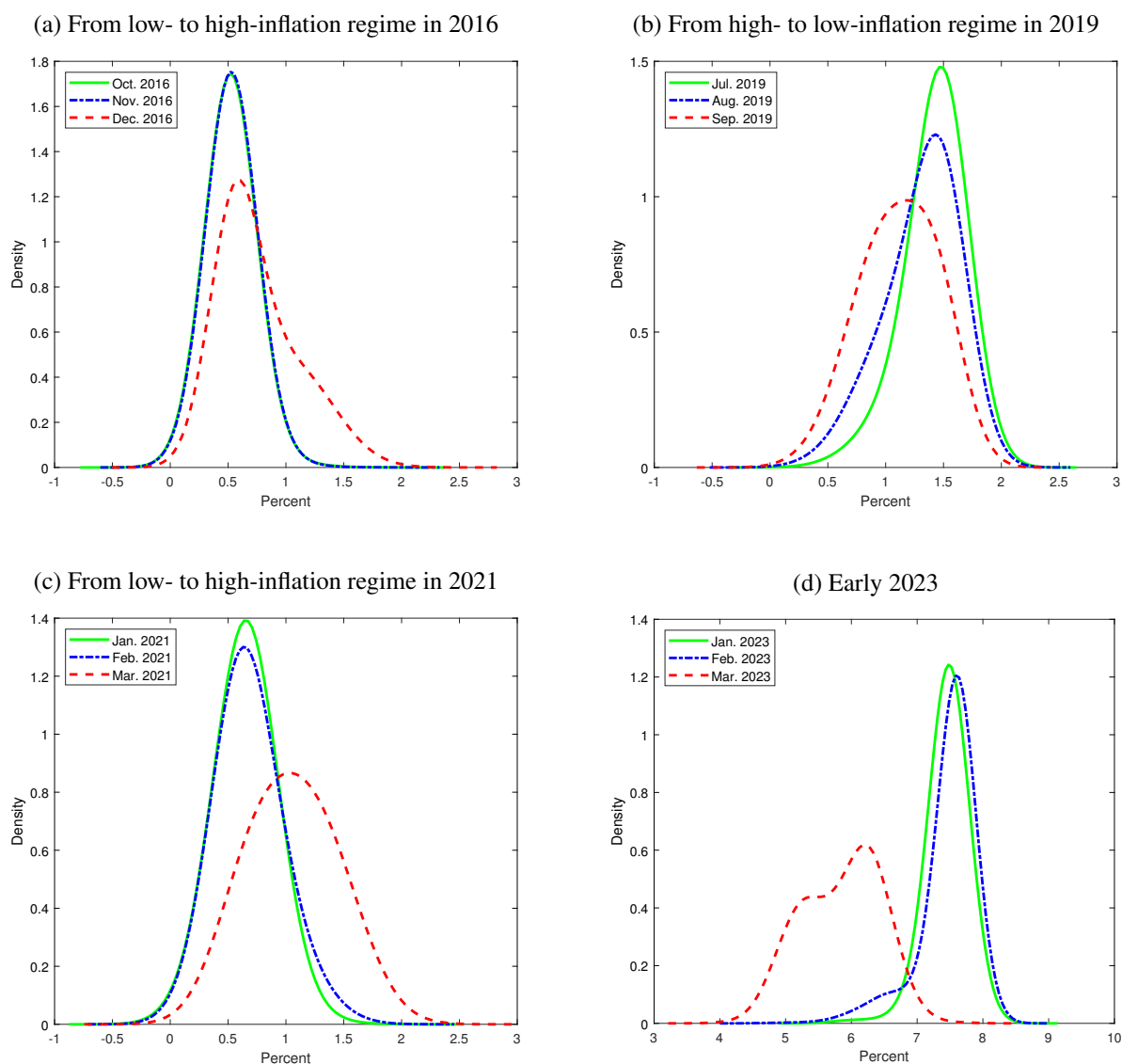
Note. The figure plots the posterior density of ICARIS for selected episodes that make reference to periods when euro area inflation transitioned from one regime to another. Low-inflation regimes are defined by a real-time probability of low inflation higher than 0.5 according to the estimates in Figure B-7. All the posterior densities shown in the figure are computed in real time, that is, by employing only information available up to the time of estimation.

positions (such as UC model), while they are based on models able to generate forecasts, generally rely on a random walk process for trend inflation. Therefore, they are not particularly informative with that respect, as trend inflation is by construction expected to stay constant at any horizon.[24] By contrast, our indicator comes with a non trivial expected future path, driven by the transition probabilities and the expected value of the persistent component.

Induced by the nonlinear nature of the estimated persistent component of inflation, our model can be used to quantify asymmetric tail risks associated with future inflation dynamics. Specifically, h-

---

[24]For this reason, medium term forecast of inflation or trend inflation associated to such indicators are rarely made explicit.

steps ahead projections of the persistent component of the i-th HICP special aggregate inflation can be computed by exploiting the Markovian property of the corresponding state variable, $s_{i,t}$, that is,

$$\mu_{i,T+h} = \bar{\mu}_{i0,\tau_{i0}}(1 - P(s_{i,T+h})) + \bar{\mu}_{i1,\tau_{i1}}P(s_{i,T+h}), \tag{16}$$

$$P(s_{i,T+h}) = \sum_{s_{i,T+h-1}} P(s_{i,T+h}|s_{i,T+h-1}, \mathbf{z}_{T+h})P(s_{i,T+h-1}), \tag{17}$$

for $h = 1, ..., H$, where $P(s_{i,T+h})$ are the regime probabilities computed with the Hamilton (1989) filter, $P(s_{T+h}|s_{T+h-1}, \mathbf{z}_{T+h})$ are the transition probabilities defined in equations (8) and (9), and $\bar{\mu}_{\kappa,\tau_\kappa}$ are the last regime-dependent means observed at the end of the sample, T, for $\kappa = \{0, 1\}$. Note that the time-varying transition probability associated with $T + h$ depends on the future value of the exogenous information, $\mathbf{z}_{T+h}$, that is, future real economic activity. Due to the complexity that forecasting real activity entails, adding to the complexity of our set-up, we take a simple approach and assume that $\hat{\mathbf{z}}_{T+h} = \mathbb{E}(\mathbf{z}_{T+h}|\Psi_T) = \mathbf{z}_T, \forall h$, where Ψ_T denotes the set of information available up to time T.[25] Since the framework is estimated in a Bayesian fashion, we are able to simulate the posterior density of $\mu_{i,T+h}$, denoted by $f(\mu_{i,T+h})$. Accordingly, h-step ahead projections of the permanent component associated to each special aggregate can be computed using equations (16)-(17), and then aggregated using Equation (15). Given the employed Bayesian estimation framework, this procedure provides the posterior density associated with each of the h-step ahead projections of the ICARIS.

Chart A of Figure 6 plots the expected path of the level of underlying inflation at a one year horizon, initiated from various points in the sample. Assessed from the point of view of the final sample date (2023:03), the ICARIS has a downward expected forward path. Moreover, the peak of the real-time ICARIS in 2023:02 confirms the view by many analysts that core inflation is set to decline in the medium term. We underline this is the outcome of a reduced-form model, that takes into account an effect of real activity on inflation, but does not explicitly take on board the monetary response to the current shock, which could subsequently be interpreted in the model as a further regime shift in inflation.

Chart B of Figure 6 plots the mounting uncertainty associated with future underlying inflation. The Mounting Uncertainty (MU) index is constructed by, first, computing the variance of the real-time projected density of ICARIS, and then, averaging those values over the horizon $h = 1, ..., H$, for each time period.[26] The MU index, that has no revisions as it is constructed in real time, can be interpreted as a timely overall assessment of the uncertainty associated with upcoming inflationary pressures. Perhaps, its most salient feature is associated with the sustained increased in uncertainty that started in mid-2021, reaching its historical maximum value in early 2022.

---

[25]Filardo (1998) proposes the inclusion of an auxiliary equation to model, and project, the exogenous information driving the transition probabilities, $\hat{\mathbf{z}}_{T+h}$. We leave such an extension for future research.

[26]We consider a one-year ahead horizon, $H = 12$. The variance of the projected density of ICARIS computed in real time is shown in Chart A of Figure B-8.

Next, we explore the skewness in the distribution of the one-year ahead projected underlying inflation. We compute what we coin as the Asymmetric Inflationary Risk (AIR) indicator, that is the average of the projected ICARIS's skewness over the entire projection horizon.[27] The AIR index can be interpreted as a summary statistics about both the direction and size of risks associated with future inflationary pressures.[28] Chart C of Figure 6 plots the AIR indicator computed in real time along with headline HICP inflation for comparison purposes. Positive values of the AIR at time t indicate right skewness in the projected underlying inflation, and implies expected upward inflationary pressures over the projection horizon, $t+1, ..., t+H$. AIR positive values are represented with red bars in the chart. Analogously, when the AIR exhibits negative values, it implies left skewness in the projected underlying inflation, which suggests upcoming downward inflationary pressures over the same projection horizon. Negative AIR values are represented by the blue bars the chart. As a general rule of thumb, if the skewness of a given distribution is between -0.5 and 0.5, it could be considered as approximately symmetric. Instead, if the skewness is higher (lower) than 0.5 (-0.5), the distribution is considered as asymmetric. Hence, for reference purposes, we include in Chart C of Figure 6 two lines associated with the values 0.5 and -0.5 of the AIR indicator.

We comment on a few of recent episodes to illustrate how the AIR can be interpreted in practice. In March 2016, the AIR took values larger than 0.5 signaling upcoming upward inflation pressures associated with a one-year-ahead projection horizon. Such pressures materialized in December 2016, when headline HICP entered a high-inflation regime. Also, in March 2019 the AIR started to report values smaller than -0.5, pointing to upcoming downward inflation pressures over the course of one year ahead. Again, such pressures did materialize when inflation switched from a high- to a low-inflation regime, in May 2020. It is worth to emphasize that the signals provided by the AIR are constructed in real time, that is, by using only information available at the time of estimation.

Focusing on the COVID period, in September 2020 the AIR already reported a value higher than 0.5, indicating an upcoming switch from low- to high-inflation regime. This transition occurred, but earlier than expected, in March 2021. Also, despite the unprecedented upward trend in inflation that started in the second half of 2021, the AIR indicator started to signaling downside risks since June 2021, implying that by mid 2022 inflation pressures would ease. However, in February 2022 the inflation landscape was exogenously changed as a consequence of the Russian invasion of Ukraine, a development our framework captures with a temporal surge in the AIR in March 2022. Since then, downward risks reported by the AIR have been predominant, and consistent with the downward trend in headline inflation observed

---

[27]We follow a similar procedure to the one used to compute the MU index, however, instead of using the variance of the projected density of ICARIS, we use its skewness. The skewness of the projected density of ICARIS computed in real time is shown in Chart B of Figure B-8.

[28]Note that the AIR index might exhibit some sensitivity to the length of the projection horizon. However, this sensitivity decreases as the projection horizon increases. The reason for this is that at longer horizons the densities of the projected ICARIS becomes symmetric, and consequently, its associated skewness approaches zero.

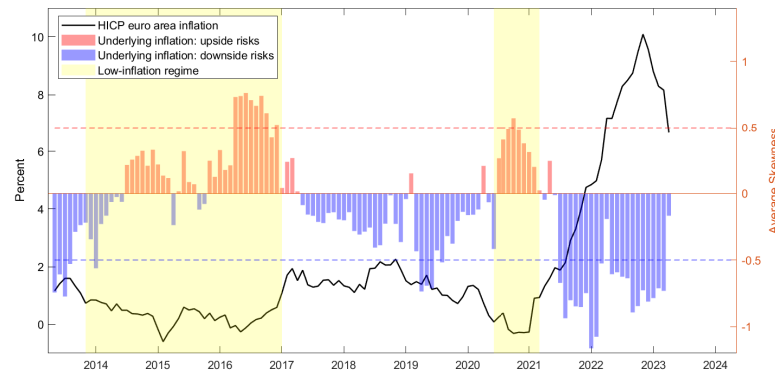## Figure 6: Outlook of Underlying Inflation in Real Time

(a) Projected Underlying Inflation
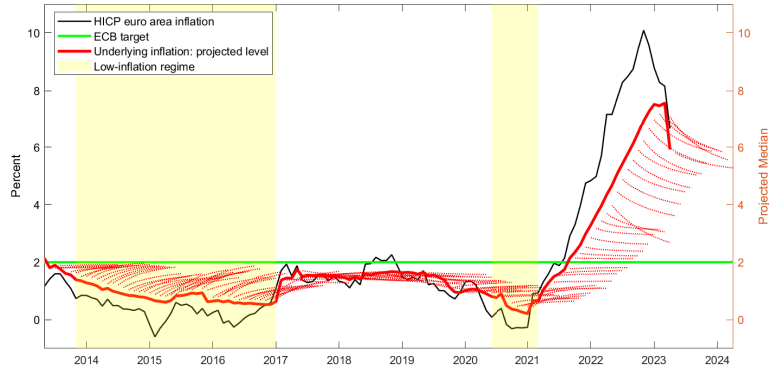
(b) Mounting Uncertainty
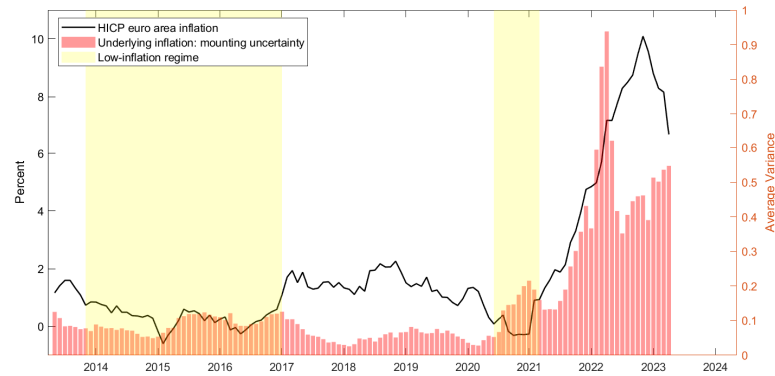
(c) Asymmetric Inflationary Risks

 Note. The projections of ICARIS in Chart (a) are obtained as a weighted average of the projections of the persistent component of inflation associated with the different special aggregates of HICP. The projections are computed based on equations (16)-(17). The Mounting Uncertainty (MU) index in Chart (b) is computed based on the average variance –over the projection horizon– of the predictive density of ICARIS, computed in real time (right axis). The Asymmetric Inflationary Risk (AIR) index in Chart (c) is computed by the average skewness –over the projection horizon– of the predictive density of ICARIS, computed in real time (right axis). The figure also plots the HICP euro area inflation with the black solid line, for reference purposes (left axis). The yellow area makes reference to low-inflation regimes, defined by a real-time probability of low inflation higher than 0.5 according to the estimates in Figure B-7. The sample covers 2013:04-2023:03.

since November 2022.

Overall, the ICARIS provides a measure of the level of underlying inflation along with its density that contains new useful information for both (i) assessing upcoming turning points in headline inflation

and (ii) measuring asymmetric risks in inflationary pressures.

4.4 The Role of Real Activity on Measuring Inflation Risks

The ability of the AIR indicator to provide accurate assessments on the risks associated with future inflation dynamics heavily depends on the information of current and past real activity, collected in $\mathbf{z}_t$, driving the probabilities of transition from one regime to another. We illustrate the role played by real activity in the quantification of inflation risks with an exercise that consists on estimating the AIR indicator using the same framework with only one change in the set of information contained in $\mathbf{z}_t$. In particular, instead of assuming that $\mathbf{z}_t$ contains information on both contemporaneous and lagged real activity, we assume that it contains only information on contemporaneous activity, that is, $\mathbf{z}_t = x_t$.

Chart A of Figure 7 plots the "alternative" AIR indicator computed by letting the transition probabilities depend on contemporaneous, and no lagged, real activity. When comparing the "benchmark" AIR indicator –plotted in Figure 6– with the "alternative" AIR indicator –plotted in Figure 7–, two main differences arise. The first, and most important, one makes reference to the timing of the inferred asymmetric risks. While the benchmark AIR indicator provides accurate inferences about the *future* direction of inflation, taking positive (negative) values about a year before headline inflation significantly rises (declines), the alternative AIR indicator provides accurate assessment on risks associated with the *current* state of inflation. That is, the alternative AIR indicator takes positive (negative) values when inflation is just about to significantly rise (decline). In this respect, while the benchmark AIR indicator can be used to provide a medium-term assessment on inflation risks, the alternative AIR indicator provides valuable information on "nowcasting" risks associated with current inflation dynamics, which can be useful in a highly uncertain environment.

The ability of the employed variable proxying real activity in helping to generate accurate inflation risk assessments can be rationalized by simply looking at their joint dynamics. Chart B Figure 7 plots the growth rate of Industrial Production along with the HICP inflation, for comparison purposes. The chart shows a leading behaviour of real activity with respect to inflation. Such a leading behaviour induces changes in the transition probabilities that help to construct projections of the persistent components of special HICP aggregates inflation rates that are highly informative about their future regime changes, and consequently, about the future underlying inflation dynamics, measured by the projected ICARIS.

## 4.5 Tracking Regime Changes in Underlying Inflation

The analysis presented in the previous sections has been centered on the construction of a measure of underlying inflation and on evaluating its properties. An additional piece of information that could also be of use for policy makers is prompt evaluation regarding whether they are operating in a regime

Figure 7: Real Activity and Underlying Inflation Risks

(a) Asymmetric Inflationary Risks: Version with Current Real Activity Only
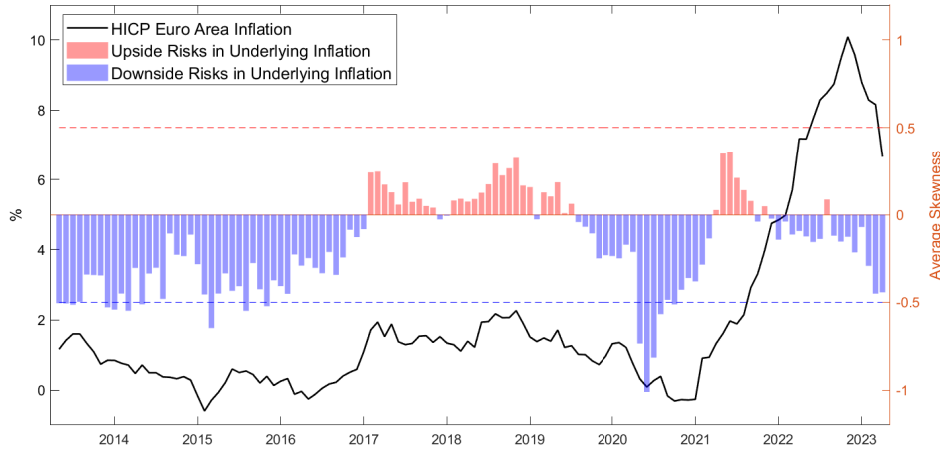
(b) Real Activity vs. Inflation
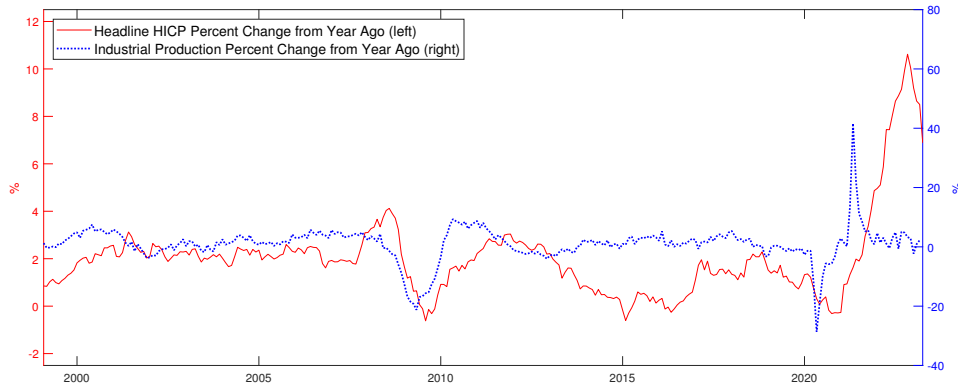
 Note. Chart A plots the measure of asymmetric inflationary risks associated with the euro area inflation, computed without using information on lagged economic activity and real time. Positive values (red bars) indicate upcoming "upside" inflationary pressures, while negative values (blue bars) suggest upcoming "downside" inflationary pressures. The HICP euro area inflation is also plotted with the black solid line, aligned with the left axis, for reference purposes. The sample covers 2013:04-2023:03. Chart B plots the year on year growth rates of HICP (left axis) and Total Industry Excluding Construction for the Euro Area (right axis). The sample covers 1999:01-2023:03.

of high or low underlying inflation. This is not a trivial task as both underlying inflation and the regime indicator are latent variables, that have to be jointly inferred.

In this section, we turn our attention to building real-time inferences on regimes of high and low underlying inflation. In doing so, we rely on our empirical framework, described in Section 2, and employ the information contained in the time-varying transition probabilities associated with each special aggregate of HICP. Specifically, we construct a weighted average of the latent variables $s_{i,t}^*$, upon which the Probit specification in Equation (7) are constructed, and let

$$S_t^* = \sum_{i=1}^N \omega_{i,t} s_{i,t}^*. \tag{18}$$

Then, we construct the probability of high-underlying inflation regime, P_t^{Core}, by employing the Bayesian draws of $S_t^{*(l)}$ generated with the estimation algorithm, as follows,

$$P_t^{Core} = \frac{1}{L} \sum_{l=1}^{L} \mathbb{I}(S_t^{*(l)} \geq 0), \tag{19}$$

where $\mathbb{I}(\bullet)$ denotes an indicator function and L is the total numbers of draws used in the Bayesian estimation procedure.

Figure 8 shows the estimated probability of high-underlying inflation regime along with, for comparison purposes, the real-time ICARIS, headline and standard (HICPX) core inflation. It results that the model identifies (in real time), over the post 2013 period two neat low inflation episodes: the first one spans the 2014 to 2017 period, and the second on spans the end-2020 to mid 2021 period. The current episode is also clearly identified from mid-2021, as a high inflation episode, with the transition having operated swiftly. Note the period 2017 to mid-2019 is not unambiguously classified by the model, reflecting diverging sectoral dynamics.

Figure 8: Real-Time Probability of High-Underlying Inflation Regime
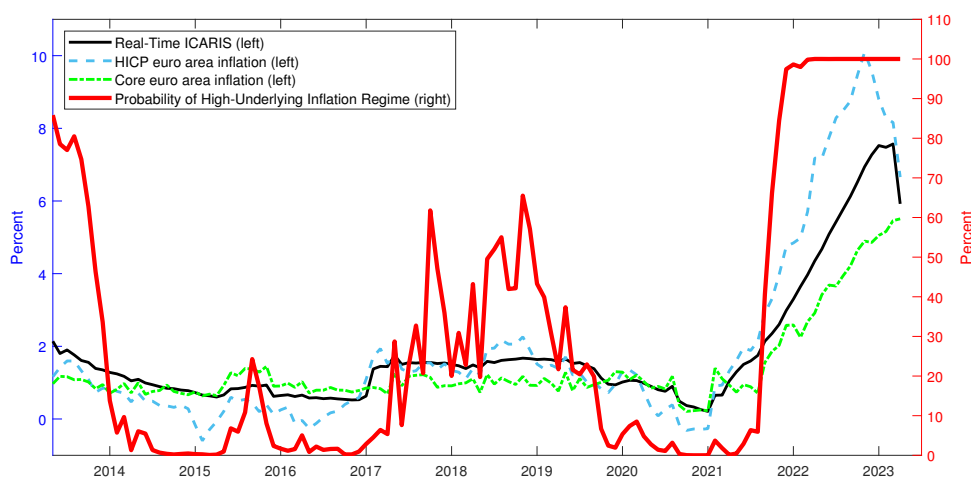
Note. The figure plots the real-time probability of high-underlying inflation regime with the solid red line (aligned with the right axis). The figure also plots the headline HICP inflation and the HICPX core inflation for references purposes (aligned with the left axis). The sample covers 2013:04-2023:03.

5   Comparing with Alternative Core Inflation Measures

We finally compare our indicator against several commonly used measures of euro area underlying inflation: HICP inflation excluding food and energy (HICPX), ECB's "Supercore" and PCCI (Persistent and Common Component of Inflation) as well as trimmed means and the weighted median measures. In this section, we also illustrate the differences that tend to arise when estimating underlying inflation with linear and nonlinear models.

5.1 Descriptive Statistics

First, we simply inspect the dynamics of the different core inflation measures, and report, in Table 2, some descriptive statistics. Figure 9 plots our measure along with the various commonly used measures of euro area core inflation, showing that our indicator stays in the range spanned by other indicators.[29]

Table 2: Measures of Underlying Inflation: Descriptive Statistics

Aggregate	Average inflation rate (%)	standard deviation	coefficient of variation	Mean absolute change
HEADLINE INFLATION	2.04	1.89	0.93	0.23
HEADLINE INFLATION EXC. FOOD AND ENERGY	1.51	0.87	0.57	0.14
PCCI OVERALL	1.99	0.96	0.48	0.10
HICP-SUPERCORE	1.71	1.01	0.59	0.11
ICARIS	1.94	1.51	0.78	0.09

Note: The statistics are based on year-on-year growth rates at the monthly frequency. The sample covers 2002:01-2023:03. The coefficient of variation is the standard deviation divided by the average inflation rate. The mean absolute change is the average of the absolute value of the first difference of each inflation measure, see Bańbura and Bobeica (2020).

The ICARIS has lower high-frequency movements than other indicators. This feature materializes in the lowest mean absolute change reported in Table 2. In this respect, the high persistence of the ICARIS facilitates the assessment of underlying inflation, especially, when facing an environment of highly volatile price developments. Also, the ICARIS displays substantial medium-range variation over the sample, reflected in the largest values of standard deviation and coefficient of variation among underlying inflation measure. This is due to the fact that the ICARIS tends to be in the lower (upper) bound of the range of core inflation measures during regimes of low (high) inflation, a feature that results from its regime-dependent nature. In fact, this feature allows the ICARIS to provide timelier assessments of turning points in inflation dynamics than the other core inflation measures. For example, during the 2014-2015 low-inflation episode, the ICARIS fell more markedly than other indicators, and stayed at the bottom of the range, providing stronger signals of deflationary risks than other indicators. By contrast during the period 2017-2019 the ICARIS located close to the upper part of the range, providing support to the progress towards reaching the inflation target.[30] Focusing on the recent period, the ICARIS jumped up earlier than other measures in 2021, and the pick up was somewhat higher in 2022. This recent signal of the ICARIS pointing to a downward reversion, as the one identified by the PCCI measure, confronts to the still increasing trajectory of other underlying inflation indicators.

When specifically comparing the ICARIS with the traditional HICPX, our measure shows more

---

[29]For comparability purposes, the chart does not report real-time but the last vintage corresponding to 2023:03, due to the unavailability of real-time vintages of some underlying inflation measures.

[30]During the second half of 2020, Germany cut value added taxes. This cut had a relatively high transitory impact on the evolution of most of the underlying inflation measures. Although, the ICARIS was relatively less affected.

Figure 9: Measures of Underlying Inflation
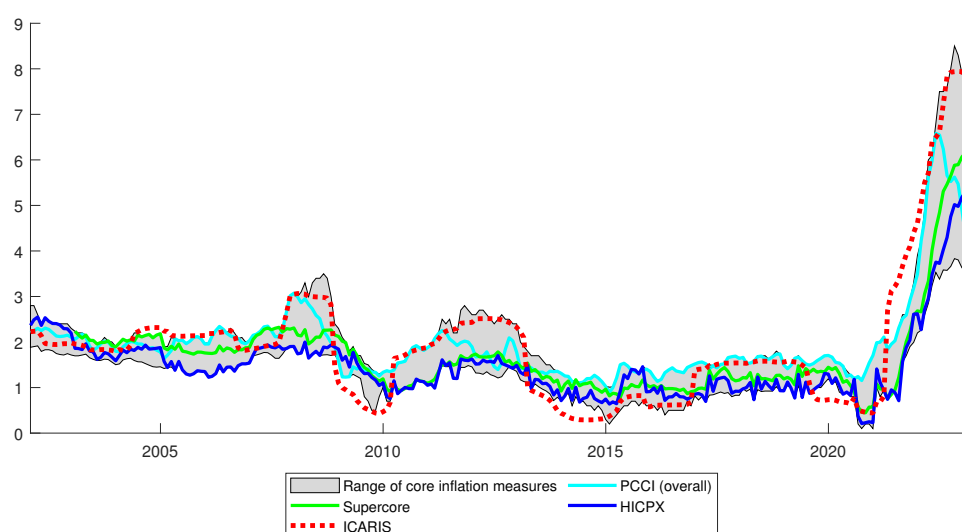
Note: The range of core inflation measures is computed taking into account the maximum and the minimum, at each month, of the year-on-year inflation rate among the following measures: HICPX; HICP excluding energy, food, travel-related items and clothing; Supercore; PCCI for HICP; PCCI for HICPX; trimmed mean 10%, trimmed mean 30%; and weighted median. All of these measures are available from the ECB Statistical Data Warehouse.

stability and is typically above the HICPX, closer to the inflation target established by the ECB.[31] The sample average of the ICARIS is 1.94%, while that of the HICPX is 1.51%, as reported in Table 2. In the context of the ECB having an objective of 2% defined in terms of the medium term value for headline HICP, we view the absence of a systematic average bias with the HICP, as one advantage of our measure over the HICPX.

5.2 Forecast Performance

An additional element we rely on to benchmark our underlying inflation measure is its forecast performance with respect to future headline inflation. In this respect, we follow the approach of Blinder and Reis (2005) and estimate the following regression:

$$\pi_{t+h} = \alpha + \beta x_t + u_{t+h}. \tag{20}$$

where π_{t+h} is the HICP year-on-year inflation in $t+h$, x_t is a measure of underlying inflation, and u_{t+h} is a forecast error. We focus on the forecast horizon $h = 12$. As in Crone, Khettry, Mester, and Novak (2013), we use a fixed-window rolling regression technique to evaluate the forecast accuracy. The motivation for doing so is, by letting the parameters of Equation (20) evolve over time, to allow for structural changes in inflation dynamics. Specifically, the first forecast regression we run uses information from

---

[31]In pursuit the price stability, the objective of the ECB was initially keeping the inflation rate below, but close to, 2% over the medium-term. In July 2021, the objective was changed to a symmetric medium-term inflation target of 2%.

January 2002 to December 2012 in order to produce the forecast of December 2013. Then, we move the fixed-window by one month and use the sample period from February 2002 to January 2013 and produce the forecast of January 2014, and so on. We follow this procedure using different measures of inflation as regressor, x_t: HICP, HICPX, trimmed mean at 10%, the weighted median, PCCI, supercore and ICARIS. The second column of Table 3 reports the pseudo-real time Root Mean Square Error (RMSE) obtained from the forecasting exercise, showing that the predictive performance of the ICARIS is in line with that of the other underlying inflation measures under consideration.

A second exercise we run follows Clark (2001) and Bańbura and Bobeica (2020). We evaluate the ability of ICARIS to predict the 12 months ahead headline inflation by estimating the following regression:

$$\pi_{t+h} - \pi_t = \gamma + \delta(x_t - \pi_t) + e_{t+h}. \tag{21}$$

As highlighted by Clark (2001), under this regression todays' gap between the measure of underlying inflation and headline inflation would predict the future change in headline inflation. Focusing on the R^2 of this regression, reported in the third column of Table 3, the ICARIS produces the largest value, implying a higher predictive content of future changes in headline inflation than that of the other measures.

Table 3: Predicting twelve month ahead inflation

Indicator	RMSE	Atractor properties		
		R^2	Intercept	Slope
HICP	2.529			
HICPX	2.665	0.069	0.454***	0.55***
Trimmed 10%	2.644	0.006	0.267**	0.455*
Weighted median	2.726	0.030	0.31***	0.447***
PCCI	2.187	0.190	0.127	1.075
Supercore	2.726	0.058	0.37***	0.53***
ICARIS	2.306	0.412	0.289***	2.706***

Note: The RMSE correspond to the forecasting exercise based on Equation (20) (see Crone, Khettry, Mester, and Novak (2013)). The attractor properties correspond the forecast exercise based on Equation (21), and make reference to the R^2 coefficients, the intercepts (γ) and slope coefficients (δ) of Equation (21). *, ** and *** denotes a 10%, 5% and 1% confidence level for a significant difference from 0, for γ, and from 1, for δ (see Bańbura and Bobeica (2020)). All the metrics are computed for the sample 2013:12-2023:03.

5.3 Linear versus Nonlinear Inflation Modelling

We turn now to illustrate the differences of our framework when compared to the random-walk alternative and to evaluate the importance of accounting for nonlinearities when modelling inflation

dynamics. For this purpose, we employ the proposed Regime-based Persistence-Noise decomposition to breakdown the *overall* headline HICP euro area inflation into its permanent and transitory fluctuations.

We decompose the euro area HICP year-on-year inflation rate into its persistent and noise components with our nonlinear model, using data from 1999:01 to 2023:03. Chart A of Figure 10 plots the persistent component of euro area inflation, showing two distinct features. First, there is clear evidence of turning points in inflation dynamics. Second, not all high-inflation regimes have the same degree of strength, neither all low-inflation regimes have the same degree of weakness. That is, each regime, either high or low, is uniquely characterized by its corresponding magnitude of inflation rate. This is an important feature that is especially relevant in the current context, when inflation in the euro area has reached historical values.

In order to evaluate the robustness of the estimated persistent component of inflation when facing a real-time environment, we reestimate the nonlinear model by using expanding windows of data for the last ten years of our sample, that is, from 2012:11 until 2023:03. Chart B of Figure 10 plots the vintages of the recursively estimated persistent component, which exhibit relatively minor historical revisions as new information is incorporated into the model. This feature suggests that the proposed framework is able to provide reliable and prompt assessments of inflation persistence.

Our methodology also performs favorable when compared to UC models. Charts C and D of Figure 10 show the estimated persistent component of inflation obtained with a "standard" UC model both with the full sample and in real-time, respectively.[32] The full-sample estimates of the persistent component obtained with the linear model are highly imprecise. This is mainly induced by the sizeable upward trend of inflation observed at the end of the sample. Due to the linearity assumption, the last "atypical" observations basically distort the entire history of the estimated persistent component, inducing a large uncertainty on the estimates. Our nonlinear framework does not suffer from these issues as the underlying persistent component is locally inferred in a piecewise fashion. Moreover, the real-time vintages of the persistent component obtained with the UC model present considerably large historical revisions, which preclude to deliver time consistent assessments of trend inflation. These results suggest that a "standard" UC linear model fails to provide a reliable estimation of the persistent component of euro area inflation.[33]

A natural comparison that arises is between the ICARIS and the persistent component obtained using only aggregate headline HICP, plotted in Charts A and B of Figure 10. Although both measures follow somewhat similar dynamics, there are important differences. The ICARIS exhibits more variability from

---

[32]The employed UC model breaks down inflation rate into persistent and temporary components, $\pi_t = \tau_t + c_t$, where the persistent component follows a random walk, $\tau_t = \tau_{t-1} + \xi_t$, and the temporary component follows an autoregressive process of order two, $c_t = \rho_1 c_{t-1} + \rho_2 c_{t-2} + \zeta_t$. The model is estimated with Bayesian methods.

[33]Similar insights are obtained when using UC models that allow for stochastic volatility in the innovations. The estimates are available upon request.

Figure 10: Persistent Component of Headline Inflation

(a) Nonlinear Model: Full Sample

(b) Nonlinear Model: Real Time Revisions

(c) Linear Model: Full Sample

(d) Linear Model: Real Time Revisions
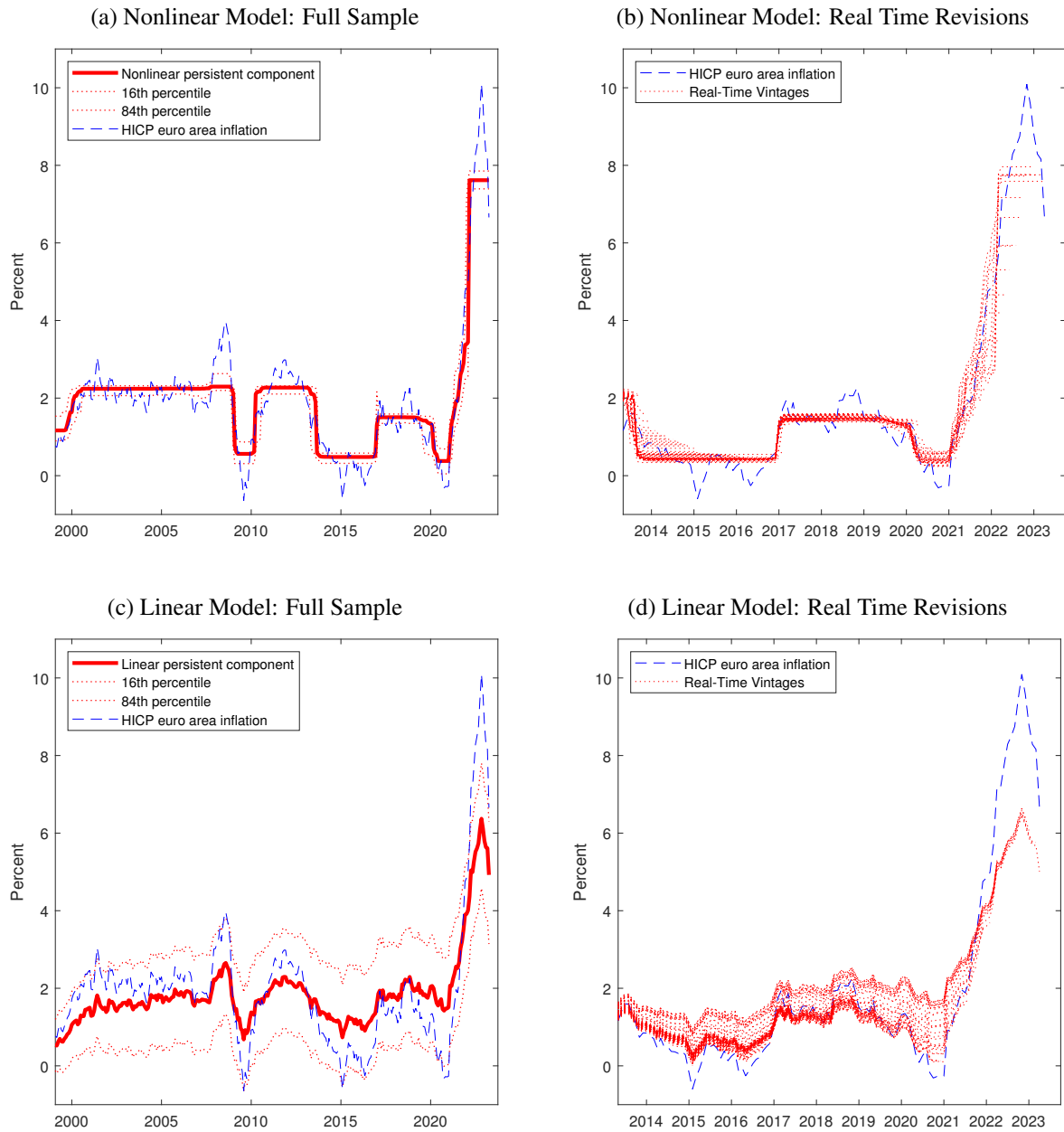
Note. Charts A and B plot the full-sample and real-time vintages of the persistent component obtained with the proposed regime-switching model, respectively. HICP inflation is decomposed into a regime-switching mean and a moving average process. Charts C and D plot the full-sample and real-time vintages of the persistent component obtained with a UC model, respectively, where inflation is decomposed into a random walk and an autoregressive process. All charts also report the HICP inflation for comparison purposes. The full-sample estimates cover 1999:01-2023:03. The real-time vintages are estimated recursively by adding one month of information at a time and covering the last ten years of data, 2013:04-2023:03.

month to month reflecting that it emerges from a weighted average across the permanent components estimated for each of the special aggregates. Moreover, the transition of the ICARIS from one inflation regime to another occurs in a smoother way than that of the persistent component of headline HICP. This smoother transition represents a key piece of information when evaluation potential internal decoupling patterns of headline HICP inflation, and also to mount a narrative on the main drivers of inflationary

pressures.

6 Concluding Remarks

We propose a new measure of core inflation based on a regime-switching framework, for the euro area. Given its inherent nonlinearity, our measure is able to shed some light on features of underlying inflation that have not be covered by existing measures. In particular, our measure is able to provide accurate real-time inferences on turning points in inflation. It can also be used to generate timely and robust inference on asymmetric risks associated with future developments of inflation. Our measure is comparable to existing measures in terms of general dynamics and ability to forecast headline inflation. Against this backdrop, we view our indicator as a relevant addition to the existing set of indicators of underlying inflation that are used to inform policy makers on latent inflationary pressures.

Several extensions of the proposed framework could be considered in order to study specifics aspects of inflation risks. One example would be the inclusion of more economic fundamentals in the set of information driving the transition probabilities ($\mathbf{z}_t$) –such as monetary policy or exchange rates–, and thus influencing risks associated with upcoming inflationary pressure. Another extension would be, as in Filardo (1998), to include auxiliary equations to jointly infer future values of the forcing variables of the regime-switching process, and potentially increase the accuracy of the inferences. We leave these possible extensions for further research.

References

ALMUZARA, M., AND A. SBORDONE (2022): "Inflation Persistence: How Much Is There and Where Is It Coming From?," Liberty Street Economics , April, Federal Reserve Bank of New York.

ALVAREZ, F., F. LIPPI, AND J. PASSADORE (2016): "Are State- and Time-Dependent Models Really Different?," in *NBER Macroeconomic Annual*, vol. 3 of *NBER Chapters*, pp. 379–457. National Bureau of Economic Research, Inc.

AMSTAD, M., S. M. POTTER, AND R. W. RICH (2014): "The FRBNY staff underlying inflation gauge: UIG," Staff Reports 672, Federal Reserve Bank of New York.

ASCARI, G., AND T. HABER (2022): "Non-Linearities, State-Dependent Prices and the Transmission Mechanism of Monetary Policy," *The Economic Journal*, 132(641), 37–57.

BAŃBURA, M., AND E. BOBEICA (2020): "PCCI - a data-rich measure of underlying inflation in the euro area," Statistics Paper Series 38, European Central Bank.

BAŃBURA, M., D. LEIVA-LEÓN, AND J.-O. MENZ (2021): "Do inflation expectations improve model-based inflation forecasts?," Working Paper Series 2604, European Central Bank.

BLINDER, A. S., AND R. REIS (2005): "Understanding the Greenspan standard," in *Proceedings-Economic Policy Symposium-Jackson Hole*, no. Aug, pp. 11–96. Federal Reserve Bank of Kansas City.

BRYAN, M. F., AND S. G. CECCHETTI (1994): "Measuring Core Inflation," in *Monetary Policy*, NBER Chapters, pp. 195–219. National Bureau of Economic Research, Inc.

CAVALLO, A., F. LIPPI, AND K. MIYAHARA (2023): "Inflation and Misallocation in New Keynesian Models," Mimeo , June, Luiss University.

CHAN, J. (2013): "Moving Average Stochastic Volatility Models with Application to Inflation Forecast," *Journal of Econometrics*, 176(2), 162–172.

CHAN, J., T. CLARK, AND G. KOOP (2018): "A New Model of Inflation, Trend Inflation, and Long-Run Inflation Expectations," *Journal of Money, Credit and Banking*, 50(1), 5–53.

CHAN, J., G. KOOP, AND S. POTTER (2016): "A Bounded Model of Time Variation in Trend Inflation, NAIRU and the Phillips Curve," *Journal of Applied Econometrics*, 31, 551–565.

CHAN, J. C. C., G. KOOP, AND S. M. POTTER (2013): "A New Model of Trend Inflation," 31(1), 94–106.

CLARK, T. E. (2001): "Comparing measures of core inflation," *Economic Review, Federal Reserve Bank of Kansas City*, 86(Q II), 5–31.

COGLEY, T. (2002): "A Simple Adaptive Measure of Core Inflation," *Journal of Money, Credit and Banking*, 34(1), 94–113.

CRISTADORO, R., M. FORNI, L. REICHLIN, AND G. VERONESE (2005): "A Core Inflation Indicator for the Euro Area," *Journal of Money, Credit and Banking*, 37(3), 539–560.

CRONE, T. M., N. N. K. KHETTRY, L. J. MESTER, AND J. A. NOVAK (2013): "Core Measures of Inflation as Predictors of Total Inflation," *Journal of Money, Credit and Banking*, 45(2-3), 505–519.

ECB (2021): "Inflation measurement and its assessment in the ECBs monetary policy strategy review," Occasional Paper Series 265, European Central Bank.

EHRMANN, M., G. FERRUCCI, M. LENZA, AND D. O'BRIEN (2018): "Measures of underlying inflation for the euro area," *Economic Bulletin Articles*, 4.

EICHENBAUM, M., N. JAIMOVICH, AND S. REBELO (2011): "Reference prices, costs, and nominal rigidities," *American Economic Review*, 101(1), 234–262.

EO, Y., AND C.-J. KIM (2016): "Markov-Switching Models with Evolving Regime-Specific Parameters: Are Postwar Booms or Recessions All Alike?," *The Review of Economics and Statistics*, 98(5), 940–949.

FILARDO, A. (1998): "Business Cycle Durations," *Journal of Econometrics*, 85, 99–123.

HAMILTON, J. D. (1989): "A New Approach to the Economic Analysis of Nonstationary Time Series and the Business Cycle," *Econometrica*, 57(2), 357–384.

KIM, C.-J., AND C. R. NELSON (1999): *State-Space Models with Regime Switching: Classical and Gibbs-Sampling Approaches with Applications*, vol. 1 of *MIT Press Books*. The MIT Press.

KLENOW, P., AND O. KRYVTSOV (2008): "State-dependent or time-dependent pricing: does it matter for recent U.S. inflation?," *The Quarterly Journal of Economics*, 123(3), 863–904.

LAGARDE, C. (2023): " The fight against inflation," *Speech, Frankfurt*, 1 June.

LALLIARD, A., AND P.-A. ROBERT (2022): "A possible new indicator to measure core inflation in the euro area," *Banque de France Bulletin*, (240), 1–11.

LANE, P. (2021): "The new monetary policy strategy: implications for rate forward guidance," *The ECB Blog*, 19 August.

——— (2023): "Underlying inflation," *Speech, Dublin*, 6 March.

LEIVA-LEÓN, D., G. PÉREZ-QUIRÓS, AND E. ROTS (2020): "Real-time weakness of the global economy: a first assessment of the coronavirus crisis," Working Paper Series 2381, European Central Bank.

LOPEZ-SALIDO, J. D., AND F. LORIA (2020): "Inflation at Risk," Finance and Economics Discussion Series 2020-013, Board of Governors of the Federal Reserve System (U.S.).

MERTENS, E. (2016): "Measuring the Level and Uncertainty of Trend Inflation," *The Review of Economics and Statistics*, 98(5), 950–967.

STOCK, J. H., AND M. W. WATSON (2007): "Why Has U.S. Inflation Become Harder to Forecast?," *Journal of Money, Credit and Banking*, 39(s1), 3–33.

——— (2016): "Core Inflation and Trend Inflation," *The Review of Economics and Statistics*, 98(4), 770–784.

VILLEROY DE GALHAU, F. (2023): "How monetary policy will defeat inflation: channels and locks," *Speech, Paris*, 17 February.

Appendix – For Online Publication Only

A Estimation Algorithm

The estimation algorithm relies on Bayesian methods and uses the Gibbs sampler, with a Metropolis step, to simulate the posterior distribution of both parameters and latent variables that characterize the model. Note that the element that links the persistence-noise decomposition associated with each special aggregate inflation is the vector $\mathbf{z}_t$. The fact that $\mathbf{z}_t$ is exogenously treated in the model makes tractable the sampling of all the elements involved in the proposed medium-size multistate Markovian framework. In particular, conditional on $\mathbf{z}_t$ the elements of the model can be independently sampled equation by equation, that is, for $i = 1, ..., n$. Accordingly, given a sample period $t = 1, 2, ..., T$, let the vectors of observed variables, latent regime, latent variable, and persistent component associated with the i-th special aggregate be defined as

$$
\begin{aligned}
\widetilde{\mathbf{Y}}_{i,T} &= [y_{i,1}\, y_{i,2} \ldots y_{i,T}], & \text{(A-1)} \\
\widetilde{\mathbf{S}}_{i,T} &= [s_{i,1}\, s_{i,2} \ldots s_{i,T}], & \text{(A-2)} \\
\widetilde{\mathbf{S}}^*_{i,T} &= [s^*_{i,1}\, s^*_{i,2} \ldots s^*_{i,T}], & \text{(A-3)} \\
\widetilde{\mu}_{i,T} &= [\mu_{i,1}\, \mu_{i,2} \ldots \mu_{i,T}], & \text{(A-4)}
\end{aligned}
$$

respectively. Each iteration of the Gibbs sampler consists of the following steps applied for $i = 1, ..., n$:

Step 1.1: Sample σ_i^2 from $\Pr(\sigma_i^2 | \widetilde{\mathbf{Y}}_{i,T}, \widetilde{\mathbf{S}}_{i,T}, \widetilde{\mathbf{S}}^*_{i,T}, \widetilde{\mu}_{i,T}, \theta_i, \lambda_i)$. To sample the variance of innovations driving the noise component, we use the conjugate Inverse-Gamma prior distribution, $IG(\eta, v)$, and generate draws from the posterior distribution

$$
\sigma_i^2 \sim IG(\bar{\eta}, \bar{v}); \tag{A-5}
$$

where

$$
\bar{\eta} = \eta + \frac{T}{2} \quad \text{and} \quad \bar{v} = v + \frac{1}{2}(\widetilde{\mathbf{Y}}_{i,T} - \widetilde{\mu}_{i,T})' \left(\mathbf{H}_{i,T} \mathbf{H}'_{i,T} \right)^{-1} (\widetilde{\mathbf{Y}}_{i,T} - \widetilde{\mu}_{i,T}), \tag{A-6}
$$

and $\mathbf{H}_{i,T}$ is a squared matrix of size equal to the number of observations in the full sample, T, that follows the same band structure as the one defined in Equation (14).

Step 1.2: Sample θ_i from $\Pr(\theta_i | \widetilde{\mathbf{Y}}_{i,T}, \widetilde{\mathbf{S}}_{i,T}, \widetilde{\mathbf{S}}^*_{i,T}, \widetilde{\mu}_{i,T}, \sigma_i^2, \lambda_i)$. By assuming a uniform prior on the interval $(-1, 1)$, $\theta_i \sim U(-1, 1)$, the conditional distribution is defined by

$$
\Pr(\theta_i | \widetilde{\mathbf{Y}}_{i,T}, \widetilde{\mathbf{S}}_{i,T}, \widetilde{\mathbf{S}}^*_{i,T}, \widetilde{\mu}_{i,T}, \sigma_i^2, \lambda_i) \propto \Pr(\widetilde{\mathbf{Y}}_{i,T} | \widetilde{\mathbf{S}}_{i,T}, \widetilde{\mathbf{S}}^*_{i,T}, \widetilde{\mu}_{i,T}, \sigma_i^2, \lambda_i, \theta_i) \mathbf{1}(|\theta_i| < 1), \tag{A-7}
$$

where $\mathbf{1}(\cdot)$ denotes an indicator function and the likelihood is given by

$$\Pr(\widetilde{\mathbf{Y}}_{i,T}|\widetilde{\mathbf{S}}_{i,T},\widetilde{\mathbf{S}}_{i,T}^*,\widetilde{\mu}_{i,T},\sigma_i^2,\theta_i,\lambda_i) = |2\pi\sigma_i^2\mathbf{H}_{i,T}\mathbf{H}_{i,T}'|^{\frac{1}{2}}\exp\left(-\frac{1}{2\sigma_i^2}(\widetilde{\mathbf{Y}}_{i,T}-\widetilde{\mu}_{i,T})'(\mathbf{H}_{i,T}\mathbf{H}_{i,T}')^{-1}(\widetilde{\mathbf{Y}}_{i,T}-\widetilde{\mu}_{i,T})\right).$$

$$\text{(A-8)}$$

We simulate the conditional density by relying a Metropolis-Hastings step. Specifically, we use the Gaussian proposal $\mathcal{N}(\widehat{\theta}_i, V_{i,\theta})$, where $\widehat{\theta}_i$ denotes the median of the conditional density, $\Pr(\theta_i|\widetilde{\mathbf{Y}}_{i,T},\widetilde{\mathbf{S}}_{i,T},\widetilde{\mathbf{S}}_{i,T}^*,\widetilde{\mu}_{i,T},\sigma_i^2,\lambda_i)$, and $V_{i,\theta}$ is the inverse of the negative Hessian evaluated at the mode. The mode $\widehat{\theta}_i$ can be obtained numerically and $V_{i,\theta}$ is computed by using finite difference methods, see Chan (2013).

Step 1.3: Sample λ_i from $\Pr(\lambda_i|\widetilde{\mathbf{Y}}_{i,T},\widetilde{\mathbf{S}}_{i,T},\widetilde{\mathbf{S}}_{i,T}^*,\widetilde{\mu}_{i,T},\sigma_i^2,\theta_i)$. Conditional $\widetilde{\mathbf{S}}_{i,T}^*$, each equation in (7) becomes an independent linear regression. Hence, to generate draws of λ_i we use the normal prior distribution $\mathcal{N}(a_\lambda, b_\lambda)$, which combined with the likelihood yields the posterior density $\mathcal{N}(\delta_{i,\lambda}, \sigma_{i,\lambda}^2)$, with

$$\sigma_{i,\lambda}^2 = \left(b_\lambda^{-1} + \widetilde{\mathbf{W}}_{i,T}'\widetilde{\mathbf{W}}_{i,T}\right)^{-1}, \qquad \text{(A-9)}$$

$$\delta_{i,\lambda} = \sigma_{i,\lambda}^2\left(b_\lambda^{-1}a_\lambda + \widetilde{\mathbf{W}}_{i,T}'\widetilde{\mathbf{S}}_{i,T}^*\right), \qquad \text{(A-10)}$$

where $\widetilde{\mathbf{W}}_{i,T} = [W_{i,1}\,W_{i,2}\,\ldots\,W_{i,T}]$ and $W_{i,t} = (1,\mathbf{z}_t,s_{i,t-1})'$. Next, conditional on λ_i, the time-varying transition probabilities, $p_i(\mathbf{z}_t)$ and $q_i(\mathbf{z}_t)$, can be generated from a Normal CDF by using equations (8) and (9).

Step 2: Sample $\widetilde{\mathbf{S}}_{i,T}$ from $\Pr(\widetilde{\mathbf{S}}_{i,T}|\widetilde{\mathbf{Y}}_{i,T},\widetilde{\mathbf{S}}_{i,T}^*,\widetilde{\mu}_{i,T},\sigma_i^2,\theta_i,\lambda_i)$. In this step, we adapt the simulation smoother proposed in Kim and Nelson (1999) for the case of time-varying transition probabilities. First, we run the Hamilton (1989) filter and save the corresponding regime probabilities—denoted by $\Pr(s_{i,t}|\mathscr{F}_{i,t})$, for $t = 1,\ldots,T$—where $\mathscr{F}_{i,t} = \{\mathbf{Y}_{i,\tau}\}_{\tau=1}^t$ denotes the sequence of data up to and including period t. Next, by letting $\widetilde{\mathbf{Z}}_{i,T} = [\mathbf{z}_1\,\mathbf{z}_2\,\ldots\,\mathbf{z}_T]$ be the vector of exogenous information driving the transition probabilities, we generate draws of the Markovian variable $\widetilde{\mathbf{S}}_{i,T}$ from the following conditional

distribution,

$$
\begin{aligned}
\Pr(\widetilde{\mathbf{S}}_{i,T}|\widetilde{\mathbf{Z}}_T,\mathscr{F}_{i,T}) &= \Pr(s_{i,1},s_{i,2},...,s_{i,T}|\widetilde{\mathbf{Z}}_T,\mathscr{F}_{i,T}) \\
&= \Pr(s_{i,T}|\widetilde{\mathbf{Z}}_T,\mathscr{F}_{i,T})\Pr(s_{i,T-1},s_{i,T-2},...,s_{i,1}|s_{i,T},\widetilde{\mathbf{Z}}_T,\mathscr{F}_{i,T}) \\
&= \Pr(s_{i,T}|\mathscr{F}_{i,T})\Pr(s_{i,T-1}|s_{i,T},\widetilde{\mathbf{Z}}_T,\mathscr{F}_{i,T})\Pr(s_{i,T-2},s_{i,T-3},...,s_{i,1}|s_{i,T},s_{i,T-1},\widetilde{\mathbf{Z}}_T,\mathscr{F}_{i,T}) \\
&= \Pr(s_{i,T}|\mathscr{F}_{i,T})\Pr(s_{i,T-1}|s_{i,T},\widetilde{\mathbf{Z}}_T,\mathscr{F}_{i,T})\Pr(s_{i,T-2}|s_{i,T},s_{i,T-1},\widetilde{\mathbf{Z}}_T,\mathscr{F}_{i,T}) \\
&\quad ...\Pr(s_{i,1}|s_{i,T},s_{i,T-1},...,s_{i,2},\widetilde{\mathbf{Z}}_T,\mathscr{F}_{i,T}) \\
&= \Pr(s_{i,T}|\mathscr{F}_{i,T})\Pr(s_{i,T-1}|s_{i,T},\widetilde{\mathbf{Z}}_T,\mathscr{F}_{i,T-1})\Pr(s_{i,T-2}|s_{i,T-1},\widetilde{\mathbf{Z}}_{T-1},\mathscr{F}_{i,T-2}) \\
&\quad ...\Pr(s_{i,1}|s_{i,2},\widetilde{\mathbf{Z}}_2,\mathscr{F}_{i,1}) \\
&= \Pr(s_{i,T}|\mathscr{F}_{i,T})\Pr(s_{i,T-1}|s_{i,T},\mathbf{z}_T,\mathscr{F}_{i,T-1})\Pr(s_{i,T-2}|s_{i,T-1},\mathbf{z}_{T-1},\mathscr{F}_{i,T-2}) \\
&\quad ...\Pr(s_{i,1}|s_{i,2},\mathbf{z}_2,\mathscr{F}_{i,1}) \\
&= \Pr(s_{i,T}|\mathscr{F}_{i,T})\prod_{t=1}^{T-1}\Pr(s_{i,t}|s_{i,t+1},\mathbf{z}_{t+1},\mathscr{F}_{i,t}). \quad\text{(A-11)}
\end{aligned}
$$

The first term on the right-hand-side of the above equation is obtained from running the Hamilton filter, computing the regime probabilities and selecting the element for $t = T$. The product in the second term is computed according to:

$$
\begin{aligned}
\Pr(s_{i,t}|s_{i,t+1},\mathbf{z}_{t+1},\mathscr{F}_{i,t}) &= \frac{\Pr(s_{i,t},s_{i,t+1},\mathbf{z}_{t+1}|\mathscr{F}_{i,t})}{\Pr(s_{i,t+1},\mathbf{z}_{t+1}|\mathscr{F}_{i,t})} \\
&\propto \Pr(s_{i,t+1}|s_{i,t},\mathbf{z}_{t+1})\Pr(s_{i,t}|\mathscr{F}_{i,t}); \quad t = T-1,T-2,\dots,1, \quad\text{(A-12)}
\end{aligned}
$$

where $\Pr(s_{i,t+1}|s_{i,t},\mathbf{z}_{t+1})$ corresponds to the time-varying transition probabilities of $s_{i,t}$, that is, $p_i(\mathbf{z}_t)$ and $q_i(\mathbf{z}_t)$, and $\Pr(s_{i,t}|\mathscr{F}_{i,t})$ is saved after running the Hamilton filter. Then, we compute

$$
\Pr(s_{i,t}=1|s_{i,t+1},\mathbf{z}_{t+1},\mathscr{F}_{i,t}) = \frac{\Pr(s_{i,t+1}|s_{i,t}=1,\mathbf{z}_{t+1})\Pr(s_{i,t}=1|\mathscr{F}_{i,t})}{\sum_{j=0}^{1}\Pr(s_{i,t+1}|s_{i,t}=j,\mathbf{z}_{t+1})\Pr(s_{i,t}=j|\mathscr{F}_{i,t})}; \quad\text{(A-13)}
$$

and generate a random number from a $U[0,1]$ distribution. If that number is less than or equal to $\Pr(s_{i,t}=1|s_{i,t+1},\mathbf{z}_{t+1},\mathscr{F}_{i,t})$, we set $s_{i,t}=1$, otherwise $s_{i,t}=0$.

Step 3: We follow the approach of Filardo (1998) and rely on the data augmentation method to generate draws of the latent variable $\widetilde{\mathbf{S}}_{i,T}^*$. In particular, given the values of $\boldsymbol{\lambda}_i$ and the inequality constraint in Equation (6), draws of $\widetilde{\mathbf{S}}_{i,T}^*$ are generated from the corresponding truncated standard Normal distribution.

Step 4: The law of motion of the regime-dependent means driving the persistent component of

Table A-1: Moments of prior distribution

Parameter	Description	Distribution	a	b
μ_{0,τ_0}	Mean inflation in low-inflation regime	$\mathcal{N}(a,b)$	0	1000
μ_{1,τ_1}	Mean inflation in high-inflation regime	$\mathcal{N}(a,b)$	1	1000
$\bar{\mu}$	Initial condition of regime-dependent means	$\mathcal{N}(a,b)$	0	1
λ_i	Probit regression coefficients	$\mathcal{N}(a,b)$	$\mathbf{0}$	$\mathbf{I}$
σ^2	Variance of innovations	$IG(a,b)$	3	2
θ	Moving average coefficient	$U(a,b)$	-1	1

Note: this table reports prior parameters.

inflation, in Equation (2), can be alternatively expressed as follows:

$$\mu_{i0,t} = (1-d_{i0,t})\mu_{i0,t-1} + d_{i0,t}\mu_{i0,\tau_0}, \tag{A-14}$$

$$\mu_{i1,t} = (1-d_{i1,t})\mu_{i1,t-1} + d_{i1,t}\mu_{i1,\tau_1}, \tag{A-15}$$

where the indicator variables $d_{i0,t}$ and $d_{i1,t}$ are defined as

$$d_{i0,t} = \Big\{ 1 \text{ when } s_{i,t}=0,\ s_{i,t-1}=1 \quad , \qquad\qquad d_{i1,t} = \Big\{ 1 \text{ when } s_{i,t}=1,\ s_{i,t-1}=0$$

The time domain $t = 1,...,T$ is partitioned into N_0 low-inflation regimes and N_1 high-inflation regimes, where a low-inflation regime is followed by a high-inflation regime, which, in turn, must be followed by another low-inflation regime. The mean μ_{i0,τ_0} represents the expected value of inflation, $\pi_{i,t}$, during the τ_0-th low-inflation regime, for $\tau_0 = 1,...,N_0$, and μ_{i1,τ_1} corresponds to the τ_1-th high-inflation regime, for $\tau_1 = 1,...,N_1$. Next, the posterior distributions defined in Equations (13) and (14) are used to generate the regime-dependent means, as described in Section 2.2.

To generate inferences on the initial condition of the regime-dependent means, defined as $\bar{\mu}$, we use the diffuse normal prior distribution $\mathcal{N}(\bar{a},\bar{b})$, which combined with the likelihood yields the posterior density $\mathcal{N}(\bar{\delta},\bar{\sigma}^2)$, with,

$$\bar{\sigma}^2 = \left(\bar{b}^{-1} + \frac{1}{\sigma^2} \right)^{-1}, \tag{A-16}$$

$$\bar{\delta} = \bar{\sigma}^2 \left(\bar{b}^{-1}\bar{a} + \frac{\pi_1}{\sigma^2} \right). \tag{A-17}$$

The time-varying means defined in equations (A-14)-(A-15) are the ones used to run the Hamilton filter in Step 2 of the algorithm.

The employed parameters of the prior distributions are reported in Table A-1. Steps 1–4 are repeated for $M = 10,000$ iterations and the first $M_0 = 2,000$ iterations are discarded to avoid the potential influence of initial conditions. The set of $M^* = 8,000$ draws constitute the posteriors densities associated with both parameters and latent variables.
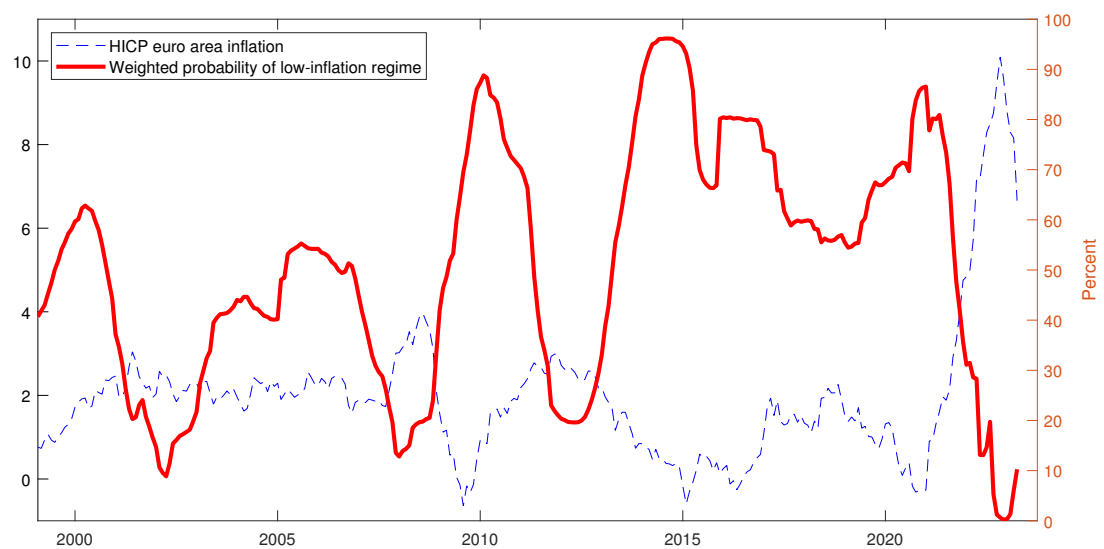
B Additional Figures

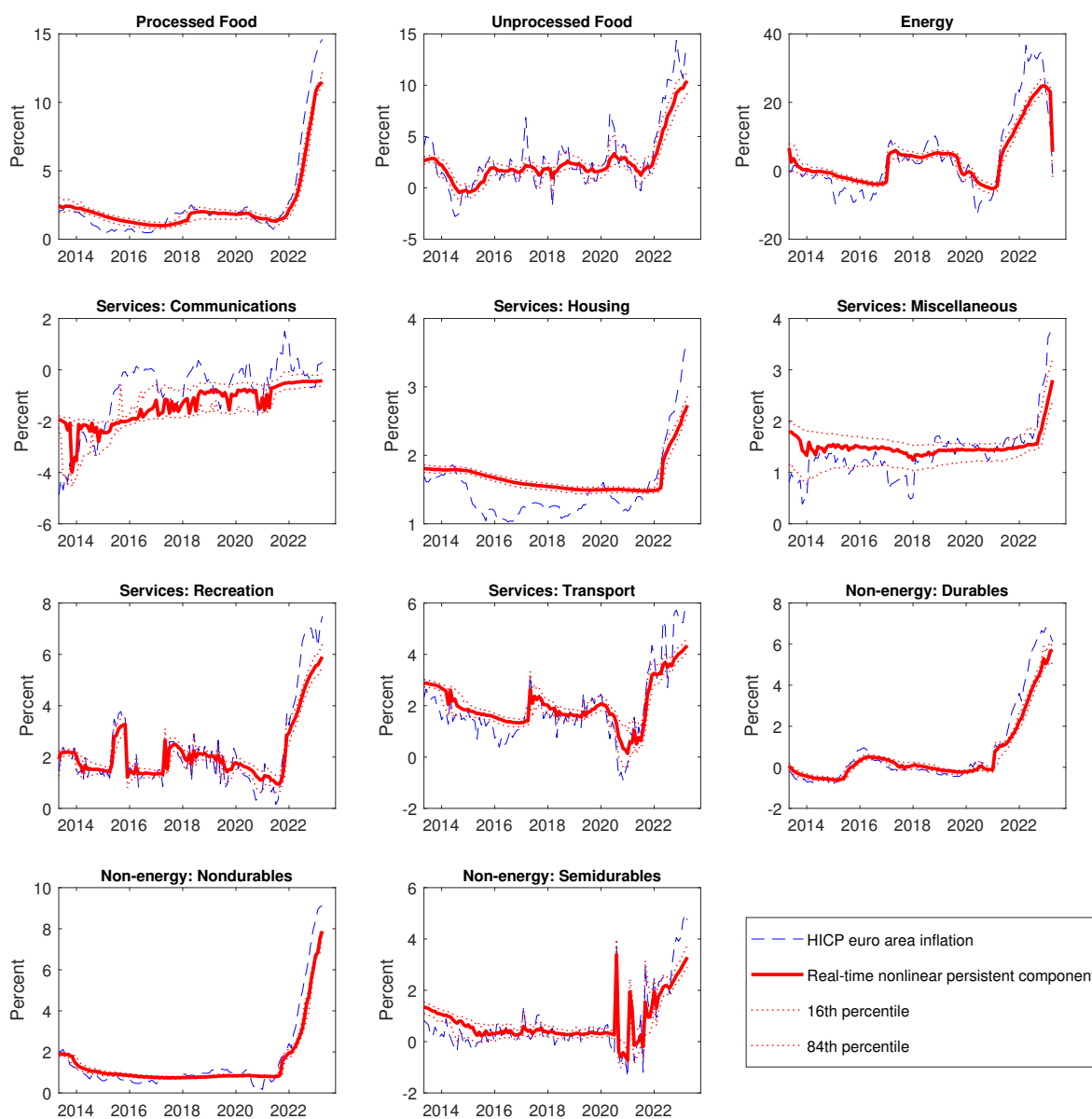Figure B-1: Probability of Low-Inflation Regime for Special Aggregates of HICP: Full Sample
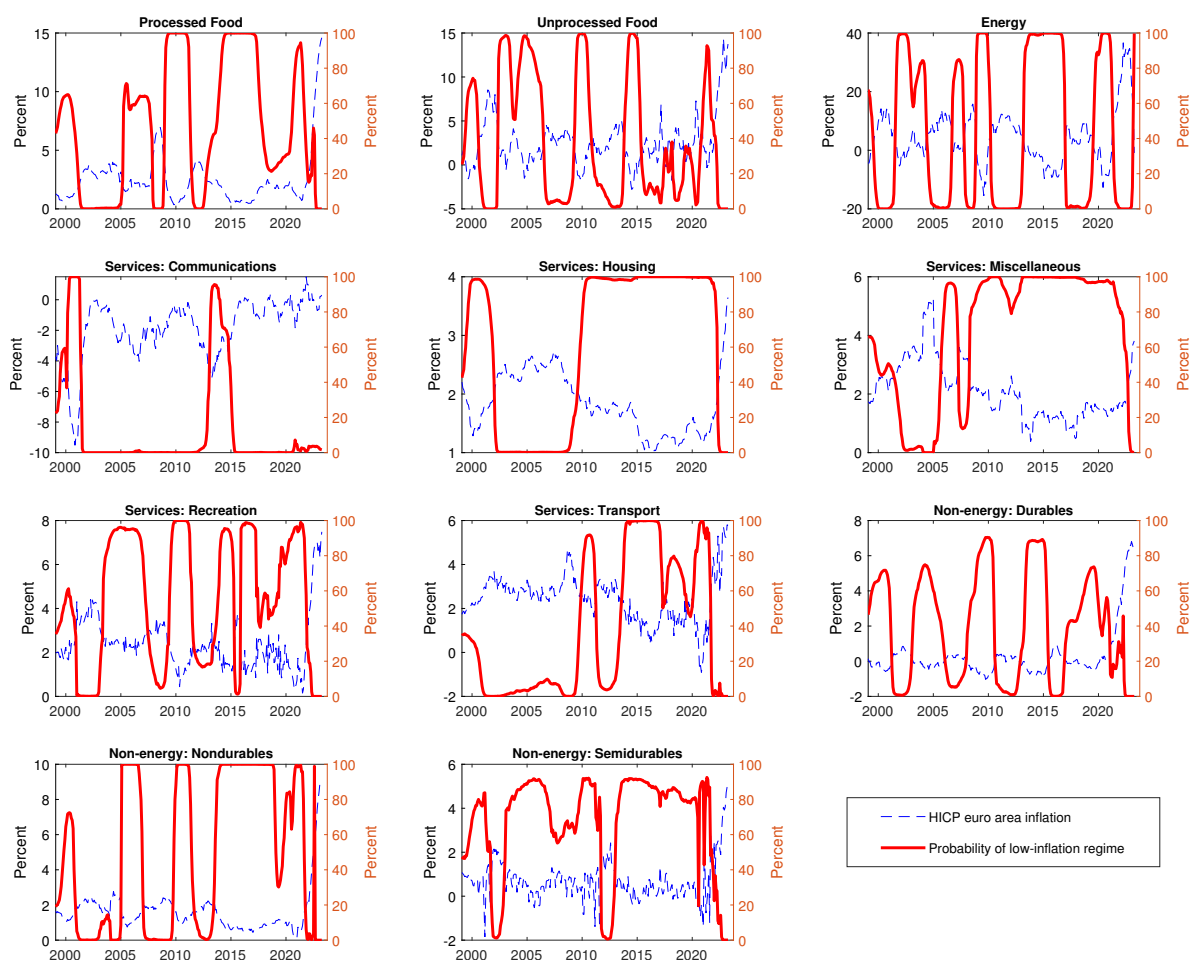
 Note. The figure plots the probability of low-inflation regime computed with the full sample (right axis). The probability is computed as the mean of the draws of the latent state, $s_{i,t}$, associated with each iteration of the employed Gibbs sampler. Each chart also plots the year-on-year growth rate of the corresponding sub-component price index for reference purposes (left axis). The sample covers 1999:01-2023:03.

Figure B-2: Weighted Probability of Low-Inflation Regime for Special Aggregates of HICP: Full Sample

 Note. The figure plots the weighted average probability of low inflation regime associated with the special aggregates of HICP (right axis). The HICP euro area inflation is also plotted for reference purposes (left axis). The sample covers 1999:01-2023:03.

Figure B-3: Persistent Component of Inflation for Special Aggregates of HICP: Real Time

Note. The figure plots the persistent component of inflation associated with the different special aggregates of HICP, computed in a real-time fashion, that is, using only the information available at the time of estimation. The persistent components are obtained with the proposed regime-switching model. Each chart also plots the year-on-year growth rate of the corresponding sub-component price index for reference purposes. The sample covers 2012:11-2023:03.

Figure B-4: Probability of Low-Inflation Regime for Special Aggregates of HICP: Real Time
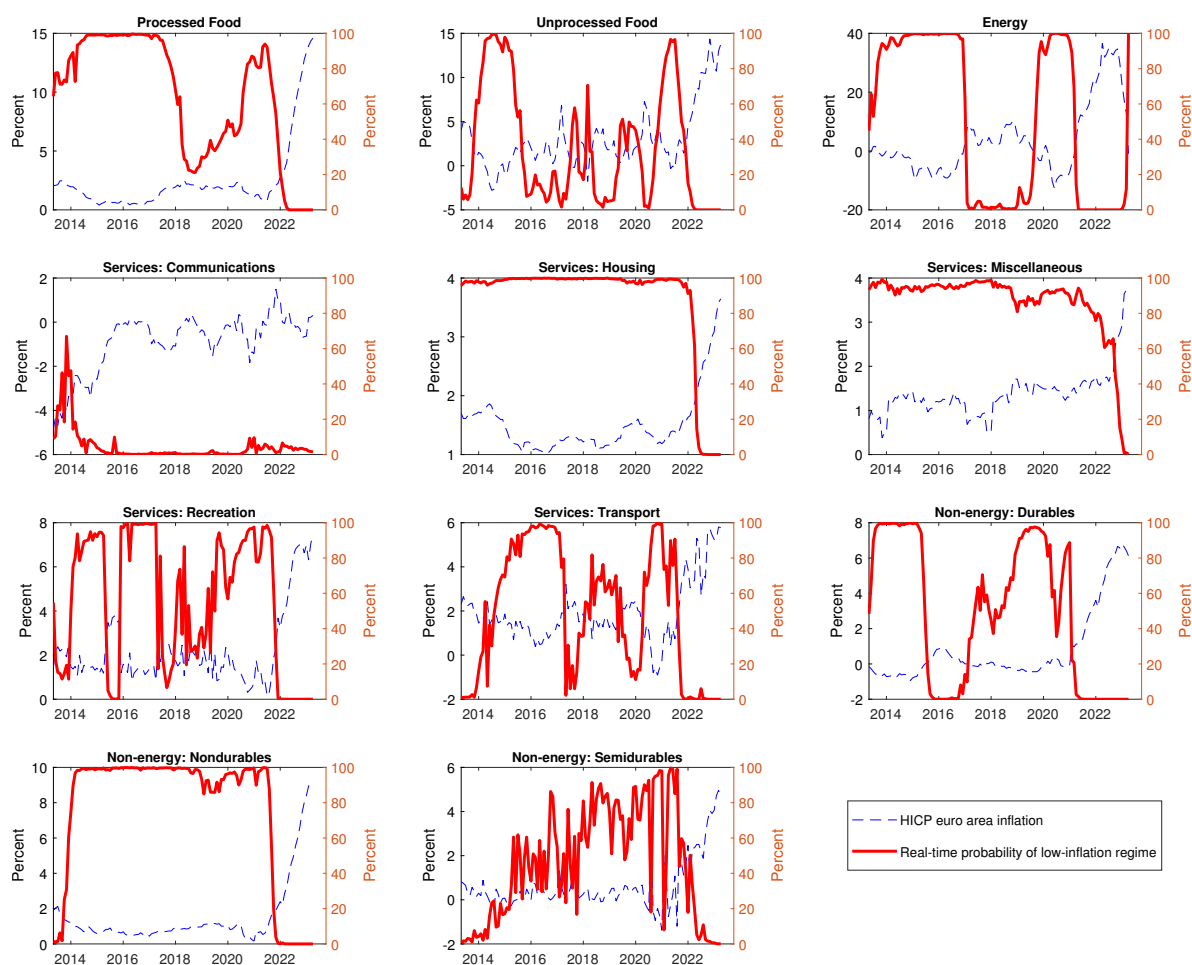
 Note. The figure plots the probability of low-inflation regime computed in a real-time fashion, that is, using only the information available at the time of estimation (right axis). The probability is computed as the mean of the draws of the latent state, s_t, associated with each iteration of the employed Gibbs sampler. Each chart also plots the year-on-year growth rate of the corresponding sub-component price index for reference purposes (left axis). The sample covers 2013:04-2023:03.

Figure B-5: Contributions of specific aggregates to HICP growth
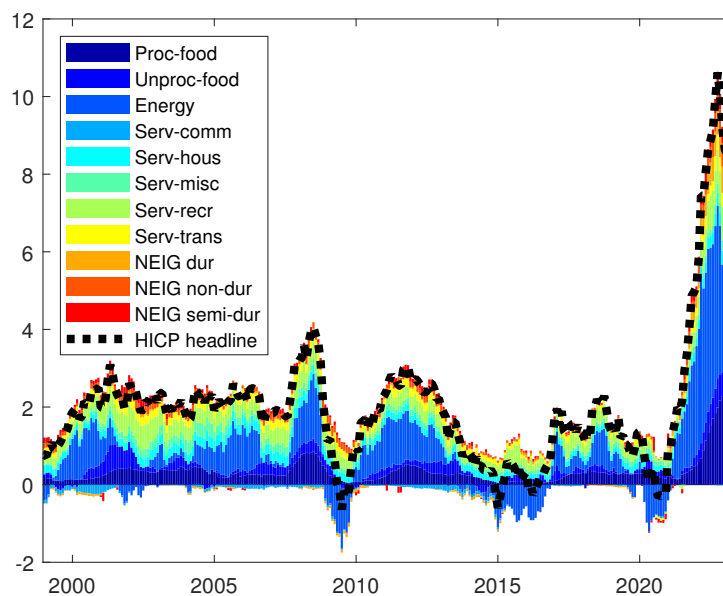
 Note. Contribution each special aggregate to the year-on-year inflation rate of headline HICP. The sample covers 1999:01-2023:03.

Figure B-6: ICARIS: Real-time Vintages
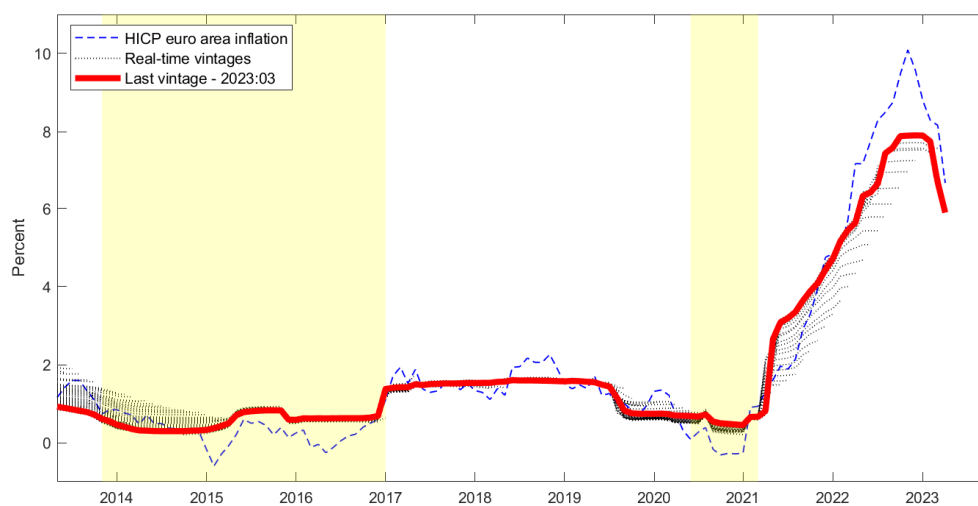
Note: The figure plots the vintages of ICARIS estimated recursively in a real-time fashion, that is using only the amount of information available at the time of estimation. The red solid line corresponds to the last vintage in the sample corresponding to 2023:03. The HICP euro area inflation is also plotted for reference purposes. The yellow area makes reference to low-inflation regimes, defined by a real-time probability of low inflation higher than 0.5 according to the estimates in Figure B-7. The sample covers 2013:04-2023:03.

Figure B-7: Headline Inflation Turning Points
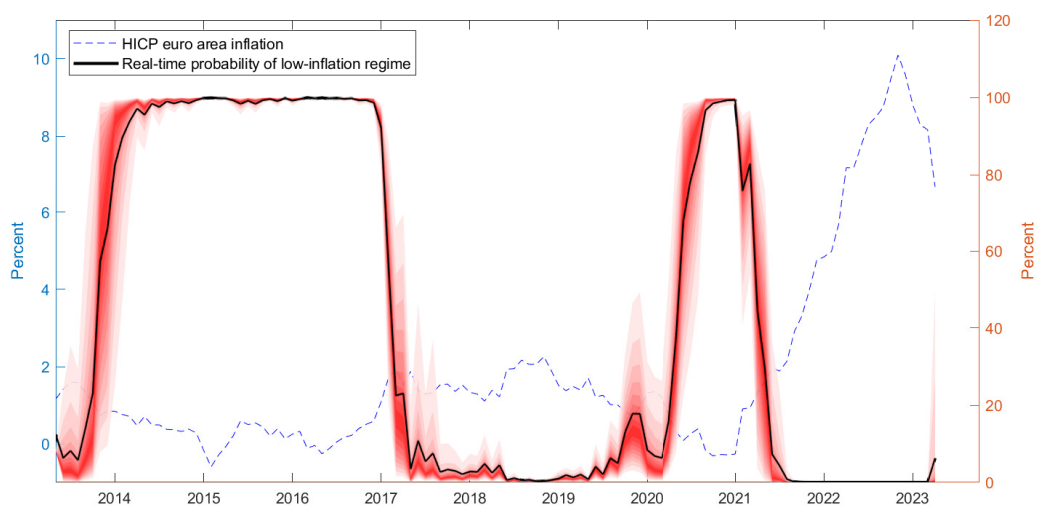
 Note. The figure plots the real-time probability of low-inflation regime (right axis), which is computed as the mean over the draws of the latent state, s_t, generated from the Gibbs sampler. The red area represents its corresponding density, which is generated by using the draws of the regime probability associated with each iteration of the Gibbs sampler. HICP euro area inflation is also plotted for reference purposes (left axis). The time span corresponds to 2013:04-2023:03.

Figure B-8: Projections of ICARIS in Real Time

(a) Variance
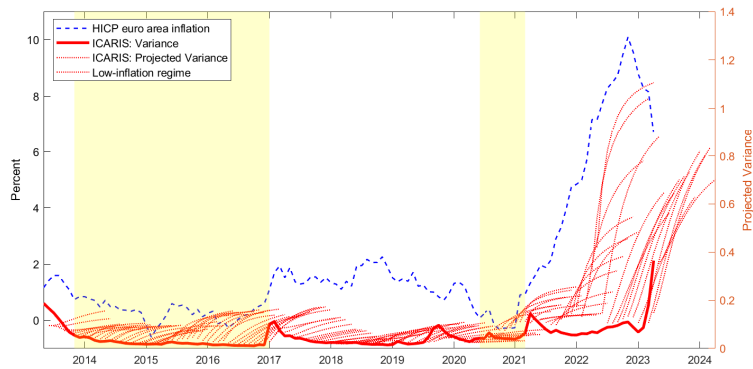
(b) Skewness
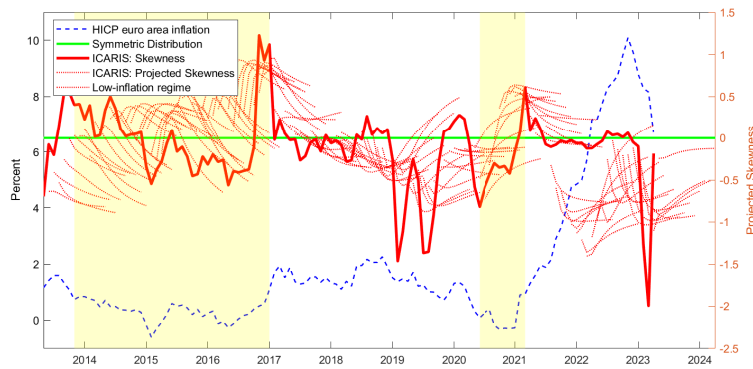
Note. Chart (a) plots the variance of the projected posterior density of the ICARIS for each point in time (right axis). Chart (b) plots the skewness of the projected posterior density of the ICARIS for each point in time (right axis). In all charts, the HICP euro area inflation is also plotted for reference purposes (left axis). The projections of density of ICARIS are obtained as a weighted average of the projections of the persistent component of inflation associated with the different special aggregates of HICP. The projections are computed based on equations (16)-(17). The yellow area makes reference to low-inflation regimes, defined by a real-time probability of low inflation higher than 0.5 according to the estimates in Figure B-7. The sample covers 2013:04-2023:03.

Hervé Le Bihan
Banque de France, Paris, France; email: herve.lebihan@banque-france.fr

Danilo Leiva-Leon
European Central Bank, Frankfurt am Main, Germany; email: danilo.leiva-leon@ecb.europa.eu

Matías Pacce
Banco de España, Madrid, Spain; email: matias.pacce@bde.es